Methods

Cell culture. Primary fibroblast lines used were 48BR and 1BR3 (control), F02/385 (Artemis null), 180BR and 495BR (LIGIV syndrome), NM720 (patient), and 709BR (mother) (8). hTERT represents immortalized derivatives. MO59K and MO59J are DNA-PK–expressing or –nonexpressing, respectively, glioblastoma cell lines (53). Cells were grown in MEM with 15% FCS, penicillin/streptomycin, and L-glutamine at 37°C and 5% CO_2. V3 (DNA-PKcs–deficient CHO cells) were cultured in α-MEM supplemented with 10% FCS, penicillin/streptomycin, and ciprofloxacin. DSB repair analysis was as described previously (8).

Immunofluorescence and immunoblotting. For immunofluorescence, anti-53BP1 or anti-γH2AX antibodies were from Millipore and Bethyl, respectively. Secondary antibodies were from Dako. Cells were fixed in 3% paraformaldehyde, 2% sucrose PBS, for 10 minutes at room temperature (RT) and permeabilized in 20 mM HEPES (pH 7.4), 50 mM NaCl, 3 mM $MgCl_2$, 300 mM sucrose, and 0.5% Triton X-100 (Sigma-Aldrich) for 2 minutes at 4°C. Primary antibody incubations were for 40 minutes at 37°C in PBS supplemented with 2% BSA (Sigma-Aldrich). Secondary incubations with anti-mouse FITC or anti-rabbit Cy3 secondary antibodies (Sigma-Aldrich) were performed at 37°C in 2% BSA for 20 minutes. Nuclei were counterstained with DAPI (Sigma-Aldrich), and coverslips were mounted in Vectashield mounting medium (Vector Laboratories). For immunoblotting, 25 or 50 μg of whole cell extracts were resolved on 7.5% PAGE gels. After transfer to PVDF membranes and blocking with 25% skim milk powder in TTBS buffer (20 mM Tris Base–HCl, pH 7.5; 150 mM NaCl; and 0.1% Tween-20), blots were incubated overnight at 4°C with anti-XLF (Eurogentec), anti-XRCC4 (Serotec), anti-KU70 (Santa Cruz), anti-KU80 (Cell Signaling), anti–DNA-LIGIV (Serotec), anti-Lis1 (Santa Cruz), or anti–DNA-PK polyclonal antibody (DPK-1; provided by S. Lees-Miller, University of Calgary, Calgary, Alberta, Canada). Blots were incubated with either rabbit, goat, or mouse secondary HRP antibodies (Dako).

DNA-PKcs kinase assay. DNA-PK kinase activity was measured using a pull-down assay (54). Briefly, whole-cell extracts from hTERT fibroblasts were mixed with 5 mg dsDNA cellulose (Sigma-Aldrich) and incubated on ice for 30 minutes at 4°C, followed by centrifugation. The pellets containing DNA cellulose–bound DNA-PKcs were washed, resuspended, and incubated with biotinylated peptide substrate supplied in the SigmaTECT DNA-PK kinase assay kit (Promega) in the presence of [γ-^{32}P] ATP for 10 minutes at 30°C. Reactions were stopped by addition of CH_3COOH, spotted onto 1.5 cm^2 phosphocellulose paper (cationic exchange paper grade P91; Whatman) and washed 3–4 times in 200 ml 15% CH_3COOH. After air drying, the signal was quantified using a STORM PhosphoImager (Molecular Dynamics/GE Healthcare).

DNA-PK sequencing. cDNA was synthesized from total RNA using random hexamer primers and SUPERSCRIPT II reverse transcriptase (Invitrogen). 9 overlapping fragments were PCR amplified using KOD polymerase (Merck Biosciences) as follows: 94°C for 2 minutes; 35 cycles of 94°C for 15 seconds, 54°C for 30 seconds, and 68°C for 90 seconds; and 68°C for 10 minutes. Each fragment was amplified 3 times in separate PCR reactions, gel purified, and sequenced in both directions using ABI BigDye Terminator Cycle Sequencing Kit V1.1 (Applied Biosystems). To confirm the exon 16 deletion, the PCR fragment covering exons 15–17 was cloned into a pGEM-5 vector, and individual clones were sequenced. Genomic DNA was extracted using a DNeasy Blood and Tissue Kit (Qiagen) and amplified in 3 overlapping fragments.

qPCR analysis. mRNA transcript levels of *PRKDC* c.10721C and c.10721T alleles in patient cells, mother cells, and 48BR control cells were quantified by the cycleave real-time PCR assay (Cycleave-qPCR; TaKaRa Co. Ltd.). *HPRT1* served as a quantification control. RNaseH-sensitive 2-color-labeled fluorescent probes that selectively recognize the *PRKDC* c.10721C and c.10721T alleles were used. qPCR results were analyzed by the ΔΔCt method. qPCR primers and probes were as follows: *PRKDC* c.10721 forward, 5′-ATAAGGAGTTTGTGGCAAGG-3′; *PRKDC* c.10721 reverse, 5′-CCAAGGCTGCATACATTC-3′; *PRKDC* c.10721C WT, (Eclipse) 5′-dAdAdG(rG)dCdAdTdTdAdAdTdA-3′ (FAM); *PRKDC* c.10721T mutant, (Eclipse) 5′-dAdAdG(rA)dCdAdTdTdAdAdTdAdAdA-3′ (ROX); *HPRT1* forward, 5′-CAGGCAGTATAATCCAAAGATG-3′; *HPRT1* reverse, 5′-ACTGGCGATGTCAATAGGA-3′; *HPRT1* probe, (Eclipse) 5′-dCdAdGdCdA(A)dGdCdT-3′ (FAM).

Plasmids and transfectants. WT DNA-PKcs expression plasmids were as described previously (42). A3574V was generated by synthesizing a portion of DNA-PKcs cDNA by multiplex PCR between the BglII (nt 10,455) and PmlI (nt 11,146) sites, including 3 nt changes within codons 3,574–3,475 (AATGCC>AACGTT) that introduce the A3574V substitution as well as noncoding substitutions that generate a novel AclI restriction site. This BglII-PmlI fragment was subcloned into a fragment of DNA-PKcs spanning the SalI site (nt 8,000) to the termination codon at nt 12,384. An Fse1 (nt 8,160) to Pml1 (nt 11,146) restriction fragment was subcloned into the complete DNA-PKcs.

Manipulation of DNA-PKcs cDNA is hampered by its size and instability. Recently, we developed an alternative expression strategy using a smaller, very low–copy number expression plasmid and the CAGG promoter. Briefly, GFP and a cloning cassette were assembled into the low-copy number plasmid pSM7 (gift of K. Yu, Michigan State University, East Lansing, Michigan, USA) between the CAGG promoter (isolated from pTriEX-2 neo; Millipore) and the bovine growth hormone poly adenylation site (isolated from PefV5His; Invitrogen). Human DNA-PKcs was cloned between unique Nhe1 and Not1 sites. cDNA was prepared from immortalized patient fibroblasts. RT-PCR was performed using primers spanning nt 1,000–2,360; 2 fragments were amplified (with and without exon 16, similar to Figure 3C). The smaller fragment was subcloned into pcr2.1 and sequenced, confirming deletion of exon 16. Plasmid DNA from this subclone as well as the CAGG-WT DNA-PKcs expression construct were prepared from bacteria lacking dcm methylase. A restriction fragment (BstZ171, nt 1,293; to SexAI, nt 1,875) spanning exon 16 was cloned from the pcr2.1 RT-PCR subclone into the CAGG-WT DNA-PKcs expression plasmid.

Complementation of primary human fibroblasts. 1BR3 control, patient, 180BR LIGIV syndrome, and mother hTERT cells were transfected with GFP-tagged full-length WT DNA-PK using Metafectine Pro Transfection Reagent (Biotex) following the manufacturer's protocol. 24 hours after transfection, cells were untreated (background) or exposed to 3 Gy IR, harvested 8 and 16 hours later, and stained for 53BP1. Only GFP^+ cells were analyzed.

Clonogenic survival assays. V3 transfectants were plated at cloning densities estimated to give scoreable colonies in the indicated dosage of zeocin. After 7 days, cell colonies were stained with 1% (w/v) crystal violet in ethanol and colony numbers were assessed. Survival was plotted as percent relative to untreated cells.

VDJ recombination assays. Extrachromosomal VDJ recombination assays were performed using the coding joint substrate pJH290 (38). V3 cells were transiently transfected with 1 μg substrate, 6 μg WT or mutant DNA-PKcs or pCMV6 vector, and 3 μg each RAG1 and RAG2 using Fugene6 transfection reagent. 48 hours later, substrate plasmids were isolated by alkaline lysis and digested with DpnI for 1 hour. Digested DNA was transformed into competent DH5α cells (Invitrogen) according to the manufacturer's instructions. Transformed cells were spread onto LB Agar plates containing 100 μg/ml ampicillin, alone or combined with 22 μg/ml chloramphenicol. Plasmid DNA from recombined pJH290 (coding joints) was isolated and sequenced.

Immunoblotting and measurement of protein kinase activity in V3 transfectants. Cell extracts were separated using 4.5% SDS polyacrylamide gels and transferred to PVDF membranes. DNA-PKcs was detected using monoclonal antibody r42-27 (gift from T. Carter, St. Johns University, New York, New York, USA). DNA-PK activity was assessed as described previously (42). Briefly, DNA-PK was pulled down onto DNA cellulose. Phosphorylation of a biotinylated peptide was assessed by capture onto SAM2 membranes (Promega Corp). Enzymatic activity was expressed as fold P-32 incorporation (bound peptide) relative to no peptide control. To assess autophosphorylation, 100 μg whole cell extracts were incubated in kinase buffer at room temperature for 5 or 30 minutes and analyzed by immunoblotting. A phosphospecific antibody was used to detect autophosphorylation at S2056 (Abcam).

Statistics. In figures where error bars are shown, results represent mean ± SD of 3 independent experiments.

Study approval. Human studies were reviewed and approved by the University of Sussex Research Governance Committee. Written informed consent was obtained from participants or their guardians.

Acknowledgments

The P.A. Jeggo laboratory is supported by the Medical Research Council, Association for International Cancer Research, and Wellcome Research Trust. The K. Meek laboratory is supported by Public Health Service grant AI048758 (to K. Meek).

Received for publication October 15, 2012, and accepted in revised form March 28, 2013.

Address correspondence to: Penny A. Jeggo, Genome Damage and Stability Centre, University of Sussex, Science Park Road, Brighton BN1 9RQ, United Kingdom. Phone: 44.273.678482; Fax: 44.273.678121; E-mail: p.a.jeggo@sussex.ac.uk. Or to: E. Graham Davies, Centre for Immunodeficiency, Great Ormond Street Hospital and Institute of Child Health, Great Ormond Street, London WC1N 3JH, United Kingdom. Phone: 44.20.7829.8834; Fax: 44.20.7813.8552; E-mail: Graham.Davies@gosh.nhs.uk. Or to: Katheryn Meek, College of Veterinary Medicine, Department of Microbiology and Molecular Genetics, and Department of Pathobiology and Diagnostic Investigation, Michigan State University, 5109 Biomedical and Physical Sciences Building, East Lansing, Michigan 48823, USA. Phone: 517.884.5361; Fax: 517.353.8957; E-mail: kmeek@msu.edu.

1. Jeggo P, Lavin MF. Cellular radiosensitivity: how much better do we understand it? *Int J Radiat Biol.* 2009;85(12):1061–1081.
2. Mahaney BL, Meek K, Lees-Miller SP. Repair of ionizing radiation-induced DNA double-strand breaks by non-homologous end-joining. *Biochem J.* 2009;417(3):639–650.
3. Soulas-Sprauel P, et al. V(D)J and immunoglobulin class switch recombinations: a paradigm to study the regulation of DNA end-joining. *Oncogene.* 2007;26(56):7780–7791.
4. Goodarzi AA, et al. ATM signaling facilitates repair of DNA double-strand breaks associated with heterochromatin. *Mol Cell.* 2008;31(2):167–177.
5. Ma Y, Pannicke U, Schwarz K, Lieber MR. Hairpin opening and overhang processing by an Artemis/DNA-dependent protein kinase complex in nonhomologous end joining and V(D)J recombination. *Cell.* 2002;108(6):781–794.
6. Riballo E, Woodbine L, Stiff T, Walker SA, Goodarzi AA, Jeggo PA. XLF-Cernunnos promotes DNA ligase IV-XRCC4 re-adenylation following ligation. *Nucleic Acids Res.* 2009;37(2):482–492.
7. Singh SK, Wu W, Wu W, Wang M, Iliakis G. Extensive repair of DNA double-strand breaks in cells deficient in the DNA-PK-dependent pathway of NHEJ after exclusion of heat-labile sites. *Radiat Res.* 2009;172(2):152–164.
8. Riballo E, et al. A pathway of double-strand break rejoining dependent upon ATM, Artemis, and proteins locating to gamma-H2AX foci. *Mol Cell.* 2004;16(5):715–724.
9. Goodarzi AA, et al. Autophosphorylation of ataxia-telangiectasia mutated is regulated by protein phosphatase 2A. *EMBO J.* 2004;23(22):4451–4461.
10. Nussenzweig A, et al. Requirement for Ku80 in growth and immunoglobulin V(D)J recombination. *Nature.* 1996;382(6591):551–555.
11. Frank KM, et al. DNA ligase IV deficiency in mice leads to defective neurogenesis and embryonic lethality via the p53 pathway. *Mol Cell.* 2000;5(6):993–1002.
12. Barnes DE, Stamp G, Rosewell I, Denzel A, Lindahl T. Targeted disruption of the gene encoding DNA ligase IV leads to lethality in embryonic mice. *Curr Biol.* 1998;8(25):1395–1398.
13. Li G, et al. Lymphocyte-specific compensation for XLF/cernunnos end-joining functions in V(D)J recombination. *Mol Cell.* 2008 Sep 5;31(5):631–640.
14. Taccioli GE, et al. Targeted disruption of the catalytic subunit of the DNA-PK gene in mice confers severe combined immunodeficiency and radiosensitivity. *Immunity.* 1998;9(3):355–366.
15. Wiler R, Leber R, Moore BB, VanDyk LF, Perryman LE, Meek K. Equine severe combined immunodeficiency – a defect in V(D)J recombination and DNA-dependent protein-kinase activity. *Proc Natl Acad Sci U S A.* 1995;92(25):11485–11489.
16. Meek K, et al. SCID in Jack Russell terriers: a new animal model of DNA-PKcs deficiency. *J Immunol.* 2001;167(4):2142–2150.
17. Meek K, et al. SCID dogs: similar transplant potential but distinct intra-uterine growth defects and premature replicative senescence compared with SCID mice. *J Immunol.* 2009;183(4):2529–2536.
18. Schwarz K, et al. RAG mutations in human B cell-negative SCID. *Science.* 1996;274(5284):97–99.
19. Schatz DG. V(D)J recombination. *Immunol Rev.* 2004;200:5–11.
20. O'Driscoll M, et al. DNA Ligase IV mutations identified in patients exhibiting development delay and immunodeficiency. *Mol Cell.* 2001;8(6):1175–1185.
21. Buck D, et al. Cernunnos, a novel nonhomologous end-joining factor, is mutated in human immunodeficiency with microcephaly. *Cell.* 2006;124(2):287–299.
22. Gatz SA, et al. Requirement for DNA ligase IV during embryonic neuronal development. *J Neurosci.* 2011;31(27):10088–10100.
23. Riballo E, et al. Identification of a defect in DNA ligase IV in a radiosensitive leukaemia patient. *Curr Biol.* 1999;9(13):699–702.
24. Moshous D, et al. Artemis, a novel DNA double-strand break repair/V(D)J recombination protein, is mutated in human severe combined immune deficiency. *Cell.* 2001;105(2):177–186.
25. van der Burg M, et al. A DNA-PKcs mutation in a radiosensitive T-B- SCID patient inhibits Artemis activation and nonhomologous end-joining. *J Clin Invest.* 2009;119(1):91–98.
26. Li G, Nelsen C, Hendrickson EA. Ku86 is essential in human somatic cells. *Proc Natl Acad Sci U S A.* 2002;99(2):832–837.
27. Wang Y, Ghosh G, Hendrickson EA. Ku86 represses lethal telomere deletion events in human somatic cells. *Proc Natl Acad Sci U S A.* 2009;106(30):12430–12435.
28. Myung K, et al. Regulation of telomere length and suppression of genomic instability in human somatic cells by Ku86. *Mol Cell Biol.* 2004;24(11):5050–5059.
29. Ruis BL, Fattah KR, Hendrickson EA. The catalytic subunit of DNA-dependent protein kinase regulates proliferation, telomere length, and genomic stability in human somatic cells. *Mol Cell Biol.* 2008;28(20):6182–6195.
30. Neal JA, Dang V, Douglas P, Wold MS, Lees-Miller SP, Meek K. Inhibition of homologous recombination by DNA-dependent protein kinase requires kinase activity, is titratable, and is modulated by autophosphorylation. *Mol Cell Biol.* 2011;31(8):1719–1733.
31. Barkovich AJ. MRI analysis of sulcation morphology in polymicrogyria. *Epilepsia.* 2010;51(suppl 1):17–22.
32. Basel-Vanagaite L, Dobyns WB. Clinical and brain imaging heterogeneity of severe microcephaly. *Pediatr Neurol.* 2010;43(1):7–16.
33. Girard PM, Kysela B, Harer CJ, Doherty AJ, Jeggo PA. Analysis of DNA ligase IV mutations found in LIG4 syndrome patients: the impact of two linked polymorphisms. *Hum Mol Genet.* 2004;13(20):2369–2376.
34. Lees-Miller SP, et al. Absence of p350 subunit of DNA-activated protein kinase from a radiosensitive human cell line. *Science.* 1995;267(5201):1183–1185.
35. Hartley KO, et al. DNA-dependent protein kinase catalytic subunit: a relative of phosphatidylinositol 3-kinase and the ataxia telangiectasia gene product. *Cell.* 1995;82(5):849–856.
36. Shin EK, Rijkers T, Pastink A, Meek K. Analyses of TCRB rearrangements substantiate a profound deficit in recombination signal sequence joining in SCID foals: implications for the role of DNA-dependent protein kinase in V(D)J recombination. *J Immunol.* 2000;164(3):1416–1424.
37. Ding Q, et al. Autophosphorylation of the catalytic subunit of the DNA-dependent protein kinase is required for efficient end processing during DNA double-strand break repair. *Mol Cell Biol.* 2003;23(16):5836–5848.
38. Hesse JE, Lieber MR, Gellert M, Mizuuchi K. Extrachromosomal DNA substrates in pre-B cells undergo inversion or deletion at immunoglobulin V-(D)-J joining signals. *Cell.* 1987;49(6):775–783.
39. Cui X, Yu Y, Gupta S, Cho YM, Lees-Miller SP, Meek K. Autophosphorylation of DNA-dependent protein kinase regulates DNA end processing and may also alter double-strand break repair pathway choice. *Mol Cell Biol.* 2005;25(24):10842–10852.
40. Douglas P, et al. The DNA-dependent protein

kinase catalytic subunit is phosphorylated in vivo on threonine 3950, a highly conserved amino acid in the protein kinase domain. *Mol Cell Biol.* 2007;27(5):1581–1591.
41. Convery E, et al. Inhibition of homologous recombination by variants of the catalytic subunit of the DNA-dependent protein kinase (DNA-PKcs). *Proc Natl Acad Sci U S A.* 2005;102(5):1345–1350.
42. Kienker LJ, Shin EK, Meek K. Both V(D)J recombination and radioresistance require DNA-PK kinase activity, though minimal levels suffice for V(D)J recombination. *Nucleic Acids Res.* 2000;28(14):2752–2761.
43. Cantagrel V, et al. Truncation of NHEJ1 in a patient with polymicrogyria. *Hum Mutat.* 2007; 28(4):356–364.
44. Shen J, et al. Mutations in PNKP cause microcephaly, seizures and defects in DNA repair. *Nat Genet.* 2010;42(3):245–249.
45. Zolner AE, et al. Phosphorylation of polynucleotide kinase/ phosphatase by DNA-dependent protein kinase and ataxia-telangiectasia mutated regulates its association with sites of DNA damage. *Nucleic Acids Res.* 2011;39(21):9224–9237.
46. Nijnik A, et al. DNA repair is limiting for haematopoietic stem cells during ageing. *Nature.* 2007;447(7145):686–690.
47. Gu Y, et al. Defective embryonic neurogenesis in Ku-deficient but not DNA-dependent protein kinase catalytic subunit-deficient mice. *Proc Natl Acad Sci U S A.* 2000;97(6):2668–2673.
48. Iliakis G. Backup pathways of NHEJ in cells of higher eukaryotes: cell cycle dependence. *Radiother Oncol.* 2009;92(3):310–315.
49. Ghosh G, Li G, Myung K, Hendrickson EA. The lethality of Ku86 (XRCC5) loss-of-function mutations in human cells is independent of p53 (TP53). *Radiat Res.* 2007;167(1):66–79.
50. Finnie NJ, Gottlieb TM, Blunt T, Jeggo PA, Jackson SP. DNA-dependent protein-kinase activity is absent in xrs-6 cells – implications for site-specific recombination and dna double-strand break repair. *Proc Natl Acad Sci U S A.* 1995;92(1):320–324.
51. Fattah KR, Ruis BL, Hendrickson EA. Mutations to Ku reveal differences in human somatic cell lines. *DNA Repair (Amst).* 2008;7(5):762–774.
52. Neal JA, Meek K. Choosing the right path: does DNA-PK help make the decision? *Mutat Res.* 2011;711(1–2):73–86.
53. Allalunis-Turner MJ, Lintott LG, Barron GM, Day RS, Lees-Miller SP. Lack of correlation between DNA-dependent protein kinase activity and tumour-cell radiosensitivity. *Cancer Res.* 1995;55(22):5200–5202.
54. Dai Y, et al. Non-homologous end joining and V(D) J recombination require an additional factor. *Proc Natl Acad Sci U S A.* 2003;100(5):2462–2467.

Gene 512 (2013) 267–274

Contents lists available at SciVerse ScienceDirect

Gene

journal homepage: www.elsevier.com/locate/gene

Uniparental disomy analysis in trios using genome-wide SNP array and whole-genome sequencing data imply segmental uniparental isodisomy in general populations

Kensaku Sasaki [a], Hiroyuki Mishima [a], Kiyonori Miura [b], Koh-ichiro Yoshiura [a,*]

[a] Department of Human Genetics, Nagasaki University Graduate School of Biomedical Sciences, Nagasaki, Japan
[b] Department of Obstetrics and Gynecology, Nagasaki University Graduate School of Biomedical Sciences, Nagasaki, Japan

ARTICLE INFO

Article history:
Accepted 19 October 2012
Available online 27 October 2012

Keywords:
Human genome
Genomic integrity
DNA repair
Gene conversion
International HapMap Project
1000 Genomes Project

ABSTRACT

Whole chromosomal and segmental uniparental disomy (UPD) is one of the causes of imprinting disorder and other recessive disorders. Most investigations of UPD were performed only using cases with relevant phenotypic features and included few markers. However, the diagnosis of cases with segmental UPD requires a large number of molecular investigations. Currently, the accurate frequency of whole chromosomal and segmental UPD in a normal developing embryo is not well understood. Here, we present whole chromosome and segmental UPD analysis using single nucleotide polymorphism (SNP) microarray data of 173 mother-father-child trios (519 individuals) from six populations (including 170 HapMap trios). For two of these trios, we also investigated the possibility of shorter segmental UPD as a consequence of homologous recombination repair (HR) for DNA double strand breaks (DSBs) during the early developing stage using high-coverage whole-genome sequencing (WGS) data from 1000 Genomes Project. This could be overlooked by SNP microarray. We identified one obvious segmental paternal uniparental isodisomy (iUPD) (8.2 mega bases) in one HapMap sample from 173 trios using Genome-Wide Human SNP Array 6.0 (SNP6.0 array) data. However, we could not identify shorter segmental iUPD in two trios using WGS data. Finally, we estimated the rate of segmental UPD to be one per 173 births (0.578%) based on the UPD screening for 173 trios in general populations. Based on the autosomal chromosome pairs investigated, we estimate the rate of segmental UPD to be one per 3806 chromosome pairs (0.026%). These data imply the possibility of hidden segmental UPD in normal individuals.

1. Introduction

Uniparental disomy (UPD) is defined as the inheritance of a chromosome pair derived only from one parent (Engel, 1980). Chromosomal UPD can occur because of gamete complementation, trisomic rescue, monosomic rescue and postfertilization error (Robinson, 2000). Uniparental heterodisomy (hUPD) is defined as the inheritance of both homologous chromosomes from one parent and occurs when bivalent chromatids fail to separate during meiosis I. Uniparental isodisomy (iUPD) is defined as the inheritance of two copies of one chromosome from one parent and may occur when sister chromatids fail to separate during meiosis II. The region of UPD may extend over an entire or segmental (interstitial or telomeric) chromosome. Segmental UPD is defined as UPD of one part of a chromosome (Kotzot, 2008), and occurs due to postzygotic somatic recombination between maternal and paternal homologues (Kotzot, 2008). Problems associated with UPD include aberrant genomic imprinting and homozygosity of autosomal recessively inherited mutations.

To maintain genome integrity, cells repair DNA damage including DNA double strand breaks (DSBs), by one of two major pathways, non-homologous end-joining (NHEJ) and homologous recombination (HR) (Wyman and Kanaar, 2006). NHEJ repair performs error-prone repair by joining DNA ends directly, independent of extensive DNA sequence homology, while HR repair performs error-free repair by utilizing the undamaged homologous sequence as the template for repair (Hartlerode and Scully, 2009). DNA damage during DNA replication can be repaired by HR using the intact sister chromatid (Sonoda et al., 2006) and inter-sister chromatid HR during S phase

Abbreviations: DSBs, double strand breaks; HR, homologous recombination; NHEJ, non-homologous end joining; UPD, uniparental disomy; hUPD, uniparental heterodisomy; iUPD, uniparental isodisomy; NGS, next-generation sequencing; WGS, whole-genome sequencing; LCLs, lymphoblastoid cell lines; SNPs, single-nucleotide polymorphisms; SNP6.0 array, Genome-Wide Human SNP Array 6.0; PartekGS, Partek Genomics Suite; INDELs, short insertions and deletions; SVs, structural variants; GATK, Genome Analysis Toolkit; CNVs, copy number variants; LTA, loss of transmitted allele; LOH, loss of heterozygosity; ROH, runs of homozygosity; QPCR, quantitative polymerase chain reaction; ESCs, embryonic stem cells.

* Corresponding author at: Department of Human Genetics, Nagasaki University Graduate School of Biomedical Sciences, 1-12-4 Sakamoto, Nagasaki 852–8523, Japan. Tel.: +81 95 819 7118; fax: +81 95 819 7121.
E-mail addresses: nell2gene@yahoo.co.jp (K. Sasaki), hmishima@nagasaki-u.ac.jp (H. Mishima), kiyonori@nagasaki-u.ac.jp (K. Miura), kyoshi@nagasaki-u.ac.jp (K. Yoshiura).

0378-1119/$ – see front matter © 2012 Elsevier B.V. All rights reserved.
http://dx.doi.org/10.1016/j.gene.2012.10.035

will not result in segmental iUPD. However, several imprinting disorders such as Beckwith–Wiedemann syndrome (BWS; OMIM #130650), Prader Willi syndrome (PWS; OMIM #176270), and Angelman syndrome (AS; OMIM #105830) can be caused by UPD. In BWS almost all patients with UPD have segmental UPD; in contrast, in PWS/AS patients mostly have UPD of the whole chromosome. In addition to those imprinting disorders, recessive hereditary disease can be caused by segmental iUPD (Kotzot, 2001; Pérez et al., 2011). Because segmental iUPD can be found in some disorders, it is possible that segmental UPD can occur in normal development without any disease phenotype. Segmental iUPD could be considered the signature of HR between maternal and paternal homologues during the early stages of embryogenesis.

UPD can be detected using microsatellite analysis (Hannula et al., 2000) and methylation testing (Baumer et al., 2001), based on a limited number of markers in the chromosomal region of interest. The advent of high throughput single nucleotide polymorphism (SNP) microarray technology has recently permitted the identification of UPD in DNA samples from clinically affected individuals (Altug-Teber et al., 2005; Pérez et al., 2011), and the number of UPD case reports is increasing (Pérez et al., 2011). To assess the clinical significance of UPD, it is necessary to document the frequency and nature of UPD in the general population. Recently, several studies reported mosaic genomic variations (copy-neutral loss of heterozygosity (LOH) or acquired UPDs, trisomies and CNVs) in blood and buccal genomic DNA samples from cancer cases and controls (Jacobs et al., 2012; Laurie et al., 2012; Rodríguez-Santiago et al., 2010). However, assessing the segmental UPD in general populations using trios and genome-wide SNP array has not been performed to date.

Two thousand cases of UPD have been reported thus far (http://www.fish.uniklinikum-jena.de/UPD.html). UPD is one of the causes of "imprinting disorders" and is found at a high rate (7% for AS and 25% for PWS: Amor and Halliday, 2008). BWS has segmental UPD11p in 20% of cases (Amor and Halliday, 2008). Until 2010, 122 cases were reported as segmental UPD, and ~65% of those cases were due to BWS and segmental paternal UPD 11p (Liehr, 2010). However, segmental UPD of other chromosomes not associated with a cytogenetically abnormal karyotype is extremely rare (Kotzot, 2001), and UPD has no effect on phenotype at many chromosomal region. Although UPD cases without clinical abnormalities have been reported in the literature, they were found by chance or were due to repeated abortions in a family with chromosomal rearrangement (Liehr, 2010). Thus, despite the increasing importance of UPD as a disease causing mechanism, the precise UPD rate, including segmental UPD, in the general population is unknown.

Little information is available regarding DNA repair in the early development of zygotes. But it is clear that segmental iUPD detected systemically in adult can be the result from inter-allelic HR during the postzygotic period to the early embryonic stage. Therefore, we attempted to identify segmental iUPD in individuals without an abnormal phenotype. To this aim, we analyzed parent-offspring trios from SNP microarray data and also whole-genome sequencing (WGS) data of genomic DNA from two trios derived from lymphoblastoid cell lines (LCLs) during the pilot 2 data of the 1000 Genomes Project (http://www.1000genomes.org/) (Altshuler et al., 2010). WGS data was used to identify shorter iUPD, because it is difficult to identify shorter segmental iUPD by SNP microarray due to limited SNP information of the whole genome.

In this paper, we evaluated the frequency of UPD in healthy normal development.

2. Materials and methods

2.1. HapMap 3 samples

We downloaded and studied a set of 170 trios (510 samples) data from SNP6.0 arrays from 5 populations in HapMap 3 (ftp://ftp.ncbi.nlm.nih.gov/hapmap/raw_data/hapmap3_affy6.0/); 159 individuals from the Centre d'Etude du Polymorphisme Humain collected in Utah, USA, with ancestry from northern and western Europe (CEU); 33 Africans with ancestry in the southwestern USA (ASW); 81 Maasai in Kinyawa, Kenya (MKK); 174 Yoruba in Ibadan, Nigeria (YRI); and 63 Mexicans with ancestry in Los Angeles, California (MXL) (Supplementary Table 1).

2.2. Genomic DNA

We attempted to identify UPD in 173 trios. Three trios (original trio 1, trio 2 and trio 3) in this study were Japanese (JPT) and were healthy volunteers (not included in HapMap samples). The three trio's genomic DNA was extracted from peripheral blood following standard protocols. Genomic DNA for two HapMap trios (CEU family ID (FID) 1463 and YRI Y117 trio) was obtained from the Coriell Institute (http://ccr.coriell.org/sections/collections/NHGRI/?SsId=11).

2.3. Microarray analysis

We performed high-resolution genome-wide SNP genotyping and DNA copy number detection using Genome-Wide Human SNP Array 6.0 (SNP6.0 array) following the manufacturer's instructions (Affymetrix, Inc., Santa Clara, California, USA). Genotyping were performed using the default parameters in the Birdseed v2 algorithm of Genotyping Console (GTC) 4.1 software (Affymetrix). As a quality control for the genotyping, Contrast QC values were calculated as implemented in the GTC 4.1, and samples used passed the recommended values for contrast QC > 0.4. Genomic positions of the SNPs corresponded to the March 2006 human genome (hg18). Copy number and allele ratio analysis was performed by Partek Genomics Suite (PartekGS) version 6.5 (Partek Inc., St. Louis, Missouri, USA). For 3 trios of healthy volunteers and 170 trios from HapMap, the copy number reference generated from the intensities of 20 normal sample profiles in our laboratory and 100 HapMap sample profiles (no overlapping 170 trios) were used, respectively. The Hidden Markov Model (HMM) method was used to detect amplified or deleted regions using PartekGS with default parameters, and required at least 5 genomic markers to obtain CNVs call. We considered the 27 possible combinations of genotypes when each of the mother/father/child in a trio had a biallelic genotype (Supplementary Table 2). UPD genotypes were identified using in-house Ruby script from trio genotyping information exported from GTC. A UPD region was defined as a set of consecutive SNPs, where all plots had the same type (paternal and maternal UPD segment) and occurred along a chromosome. We used the criteria of a minimum of 6 consecutive UPD SNPs, with segments extending over 200 kilo bases (kb). In this study, we focused on the autosome, and chromosome X only when the offspring in the trio was a daughter. We visualized tracts of paternal uniparental inheritance (UPI-P), maternal uniparental inheritance (UPI-M), biparental inheritance (BPI), MI-S, single Mendelian inconsistencies (MI-S), double Mendelian inconsistencies (MI-D) and not informative (NI) in biallelic SNP data from trios using PartekGS'SNPtrio. Current software does not distinguish between homozygous and hemizygous states. In addition, it is known that UPD type genotypes can result from the loss of transmitted allele (LTA) (Ting et al., 2007). LTA was defined as a phenomenon in which the transmitted allele is lost (due to deletion or UPD) in the parent after the transmission to a normal child (Redon et al., 2006). Therefore, the putative UPD genotype overlapping with CNVs in trios confirmed using BEDtools (version 2.12.0) (Quinlan and Hall, 2010). The distinction between the segmental UPD as opposed to homozygosity due to small deletion is difficult to determine just by inspection of the SNP array data alone. To exclude false segmental UPD due to undetectable small CNVs, we adopted a cutoff value of a length of 200 kb or smaller. Finally, we confirmed whether known imprinting genes were present in the identified segmental UPD region. Imprinting

genes are based on Geneimprint (http://www.geneimprint.com/site/genes-by-species.Homo+sapiens.imprinted-All).

2.4. Next-generation sequencing (NGS) data

HapMap CEU 1463 and YRI Y117 trios were sequenced using multiple platforms, as described elsewhere (Altshuler et al., 2010). We downloaded BAM files (aligned to the NCBI36 reference genome using Maq v0.7) of two trios (CEU and YRI) sequenced using Illumina Genome Analyzer I, II and IIx in the 1000 Genomes Project pilot 2 (ftp://ftp-trace.ncbi.nih.gov/1000genomes/ftp/pilot_data/data/) with high coverage. We focused on the autosomal and X chromosomes. Each included one offspring (daughter), father and mother: CEU daughter NA12878, father NA12891 and mother NA12892; and YRI daughter NA19240, father NA19239 and mother NA19238.

2.5. NGS bioinformatics

After downloading the BAM files, duplicate reads from samples were identified and removed using Picard (version 1.38) (http://picard.sourceforge.net/). Base quality scores were recalibrated and reads were locally realigned with the Genome Analysis Toolkit (GATK) (version 1.0.5974) (DePristo et al., 2011; McKenna et al., 2010). Coverage statistics were calculated as default using GATK'DepthOfCoverageWalker. The diploid consensus sequences and variants for autosomal and X chromosomes were obtained by the 'EMIT_ALL_CONFIDENT_SITES (using -stand_call_conf 50.0 and -stand_emit_conf 10.0)' command of the GATK'UnifiedGenotyper. SNPs and short insertions and deletions (INDELs) were detected with the GATK's UnifiedGenotyper according to the Best Practice Variant Detection with the GATK v2 (http://www.broadinstitute.org/gsa/wiki/index.php/Best_Practice_Variant_Detection_with_the_GATK_v2). SNPs and INDELs were then filtered for the removal of low quality variants with GATK's VariantFiltrationWalker tools. We filtered out any SNPs matching the following criteria: greater than 10% of aligned reads included at the site have a mapping quality of 0 (MAPQ0), or overlaps INDELs, or DP > 100 || MQ0 > 40 || SB > −0.10. We filtered out any INDELs matching the following criteria: greater than 10% of aligned reads included at the site have a mapping quality of 0 (MAPQ0), or SB >= −1.0, QUAL < 10. Identified SNPs were annotated based on the dbSNP132 with ANNOVAR (Wang et al., 2010). Once the trio genotypes were determined, we extracted any iUPD genotypes that did not comply with the rules of Mendelian inheritance.

Filters were applied to exclude genomic regions in which false positive iUPD calls might be picked up. Since some genome regions are problematic for mapping and assembly, including regions of CNV in the each daughter, a putative iUPD call was not attempted in these regions (Altshuler et al., 2010; Conrad et al., 2011). We used the following filters: Simple Repeats, Segmental Duplications, CNV regions (Conrad et al., 2010; Kidd et al., 2008; McCarroll et al., 2008; Mills et al., 2011), and read depth (sites where at least one trio member has no mapped Illumina reads). BEDTools was used to confirm the intersections between putative iUPD genotypes and above-mentioned regions (Quinlan and Hall, 2010). Other annotations are based on The National Center for Biotechnology Information (NCBI; http://www.ncbi.nlm.nih.gov/) and The University of California Santa Cruz (UCSC; http://genome.ucsc.edu/) databases. Finally, we required each genotype in a trio to have qualities GQ40 or greater for more efficient identification of the true iUPD genotypes.

2.6. Capillary sequencing

Validation experiments were performed on the DNA extracted from LCLs in each trio by a standard capillary sequencing approach. For CEU 1463 and YRI Y117 trios, primers were designed for 140 and 178 sites, respectively. We designed PCR primers using PrimerZ (http://genepipe.ngc.sinica.edu.tw/primerz/beginDesign.do) (Tsai et al., 2007) or Primer3Plus (http://www.bioinformatics.nl/cgi-bin/primer3plus/primer3plus.cgi) (Untergasser et al., 2007). Primers for each data set are provided in Supplementary Table 3.

2.7. Quantitative polymerase chain reaction (qPCR)

qPCR analysis was performed to measure the genomic copy number using a LightCycler 480 (Roche Diagnostics, Basel, Switzerland) and the Thunderbird SYBR qPCR Mix (Toyobo Co., Ltd.) according to the manufacturer's experimental protocol. Two sets of primers, zinc finger protein 80 (*ZNF80*) and G protein-coupled receptor 15 (*GPR15*) (D'haene et al., 2010), were used as references for quantification. Data analysis was performed with the second derivative maximum method of LightCycler 480 software (version 1.5.0.39) (Roche Diagnostics). qPCR amplification was carried out in triplicate. Primers for target regions were designed to surround the putative iUPD genotype by PrimerZ. Primers for each data set are provided in Supplementary Table 3.

3. Results

3.1. A whole chromosomal and segmental UPD analysis in 173 trios using SNP6.0 array

To investigate whole chromosome and segmental UPD in general populations using SNP6.0 array data, we examined the genotypes of the 173 trios that included 3 JPT trios in Nagasaki and 170 HapMap trios. Screening of UPD segments identified 46 putative segments (Table 1). A whole chromosomal UPD was not found in any chromosome except the Y chromosome in all samples tested. To rule out false segmental UPD due to CNVs and LTAs, we performed CNV analysis (Supplementary Table 4) and then cross-referenced with regions of putative segmental UPD in each trio (Table 1). As a result, we identified 24 CNVs, 21 LTAs (18 results from CNV and 3 possible copy number neutral LOH in the investigated parent's genome) (Supplementary Figs. 1–3) and 1 obvious segmental iUPD (Table 1). This one segmental iUPD indicated a paternal iUPD range from p-terminal to physical position 8,202,065 on chromosome 17p13.3-13.1 (about 8.2 mega bases (Mb)) in NA19918 (HapMap ASW FID 2431) (Fig. 1).

3.2. Base calling and detection of iUPD genotype

We investigated the possibility of the shorter segmental iUPD being undetectable by SNP6.0 array in the human genome using sequence data with a high coverage by Illumina platform during the pilot phase 2 of the 1000 Genomes Project. For each of the trios, we called the genotype of the three genomes independently using the GATK framework. In the CEU trio (NA12878, NA12891 and NA12892), mapped sequence coverage of 31.9×, 30.3× and 25.6×, respectively, and 2.32, 2.33 and 2.31 gigabases (Gb) of accessible genome included 2.85, 2.85, 2.79 million SNPs. In the YRI trio (NA19240, NA19239 and NA19238), mapped sequence coverage of 33.4×, 24.5× and 20.6×, respectively, and 2.36, 2.30 and 2.23 Gb of accessible genome included 3.60, 3.40 and 3.10 million SNPs. The accessible genome per CEU and YRI trio set were 2.24 Gb and 2.14 Gb, respectively. Statistics for each data set are provided in Table 2. Of these accessible genomes in each trio set, in the CEU 1463 and YRI Y117 trios, 1,094 and 1,474 putative iUPD genotypes were selected, respectively (Fig. 2). To exclude false iUPD genotypes, we filtered out the putative iUPD genotypes overlapping with regions of the simple repeats and segmental duplications and previously reported CNVs in the trio's daughter (Supplementary Tables 5 and 6). As a result, we identified 502 and 965 putative iUPD genotypes in the CEU 1463 and YRI Y117 trio, respectively (Fig. 2).

Table 1
Summary of putative segmental UPD segments in 173 trios detected by SNP6.0 array data analysis. Chr, chromosome; CNV, copy number variant; ND, not detectable; LTA, loss of transmitted allele; iUPD, uniparental isodisomy; LOH, loss of herozygosity.

Chr	Start position	End position	Population	HapMap FID	Sex	UPD type	Mother CNV	Father CNV	Child CNV	Result	UPD probe number	Length (bp)
11	51,078,178	51,359,581	ASW	2368	XY	Paternal	CNV	ND	ND	LTA	7	281,404
17	6,689	8,202,065	ASW	2431	XY	Paternal	ND	ND	ND	Paternal iUPD	301	8,195,377
7	119,133,278	119,393,868	ASW	2427	XY	Maternal	ND	CNV	CNV	CNV	8	260,591
6	137,300,451	143,369,018	CEU	1423	XX	Paternal	CNV	ND	ND	LTA	122	6,068,568
5	107,513,060	107,716,753	CEU	1350	XY	Paternal	ND	ND	CNV	CNV	15	203,694
8	14,677,944	15,701,490	CEU	1375	XX	Paternal	CNV	ND	CNV	CNV	64	1,023,547
7	88,496,196	88,887,792	CEU	1330	XY	Paternal	CNV	ND	CNV	CNV	15	391,597
2	85,751,279	88,861,509	CEU	1330	XX	Paternal	CNV	ND	ND	LTA	34	3,110,231
12	129,502	131,942,726	CEU	1444	XY	Paternal	ND	ND	CNV	CNV	825	131,813,225
11	81,131,219	81,387,538	CEU	1447	XX	Paternal	CNV	ND	CNV	CNV	11	256,320
22	20,825,481	21,201,922	CEU	1459	XY	Paternal	CNV	ND	ND	LTA	7	376,442
X	28,498,460	31,437,190	CEU	1463	XX	Paternal	CNV	CNV	ND	LTA	34	2,938,731
4	118,785,685	119,509,766	CEU	1340	XX	Maternal	ND	CNV	ND	LTA	16	724,082
12	33,468,716	34,188,071	CEU	1345	XX	Maternal	ND	CNV	ND	LTA	9	719,356
22	20,784,680	21,191,527	CEU	1420	XX	Maternal	ND	CNV	ND	CNV	11	406,848
X	276,282	154,127,693	CEU	1349	XX	Maternal	ND	ND	CNV	CNV	2,170	153,851,412
15	21,205,648	45,731,444	CEU	1377	XY	Maternal	ND	CNV	ND	LTA	85	24,525,797
18	65,224,346	76,085,336	CEU	1328	XX	Maternal	ND	CNV	ND	LTA	369	10,860,991
22	20,927,130	21,243,931	CEU	1330	XY	Maternal	ND	CNV	ND	LTA	8	316,802
1	206,304,300	246,785,226	CEU	1330	XX	Maternal	ND	CNV	ND	LTA	144	40,480,927
17	69,586,313	70,111,013	CEU	13281	XY	Maternal	CNV	ND	CNV	CNV	12	524,701
X	140,182,100	140,575,068	CEU	1354	XX	Maternal	ND	CNV	CNV	CNV	18	392,969
22	20,718,086	21,107,920	CEU	1358	XY	Maternal	ND	ND	CNV	CNV	15	389,835
1	144,979,429	145,700,719	CEU	1459	XX	Maternal	ND	ND	ND	LTA (putative LOH in father)	51	721,291
1	236,789,304	246,590,204	CEU	1459	XX	Maternal	ND	ND	ND	LTA (putative LOH in father)	396	9,800,901
11	114,231,222	134,235,117	CEU	1463	XY	Maternal	ND	ND	ND	LTA (putative LOH in father)	543	20,003,896
13	82,217,462	83,042,185	MXL	M019	XX	Maternal	ND	ND	CNV	CNV	9	824,724
6	140,718,454	141,182,824	MXL	M027	XX	Maternal	ND	CNV	CNV	CNV	9	464,371
X	4,726,561	145,198,977	MKK	2596	XX	Paternal	CNV	CNV	ND	LTA	611	140,472,417
22	20,909,341	21,181,447	MKK	2699	XY	Paternal	ND	ND	CNV	CNV	7	272,107
11	55,060,441	55,440,561	MKK	2588	XX	Maternal	ND	CNV	CNV	CNV	8	380,121
5	110,517,276	110,787,436	MKK	2634	XY	Maternal	ND	CNV	CNV	CNV	17	270,161
9	11,947,750	12,155,758	MKK	2634	XY	Maternal	ND	CNV	CNV	CNV	11	208,009
22	24,042,173	24,292,988	MKK	2634	XY	Maternal	ND	CNV	ND	LTA	9	250,816
1	245,373,155	247,137,334	YRI	Y014	XX	Paternal	ND	ND	CNV	CNV	66	1,764,180
3	136,397,878	137,151,871	YRI	Y014	XX	Paternal	CNV	ND	ND	LTA	10	753,994
11	329,969	26,983,000	YRI	Y014	XX	Paternal	ND	ND	CNV	CNV	263	26,653,032
X	2,386,344	25,622,488	YRI	Y014	XX	Paternal	CNV	ND	ND	LTA	81	23,236,145
19	22,821,274	23,413,380	YRI	Y074	XY	Paternal	ND	ND	CNV	CNV	7	592,107
7	119,175,698	119,393,868	YRI	Y038	XX	Paternal	CNV	ND	CNV	CNV	8	218,171
12	73,201,200	91,388,277	YRI	Y112	XY	Paternal	CNV	ND	ND	LTA	70	18,187,078
1	22,392,010	28,325,476	YRI	Y003	XY	Maternal	ND	ND	CNV	CNV	97	5,933,467
15	20,318,185	20,773,725	YRI	Y009	XY	Maternal	ND	CNV	CNV	CNV	11	455,541
22	24,012,780	24,238,616	YRI	Y071	XY	Maternal	ND	CNV	CNV	CNV	10	225,837
13	18,759,817	19,002,511	YRI	Y039	XY	Maternal	ND	CNV	ND	LTA	9	242,695
2	151,462,078	153,347,758	YRI	Y048	XY	Maternal	ND	CNV	ND	LTA	36	1,885,681

3.3. GQ threshold and filtering for iUPD genotypes

Our approach was simple and would allow false iUPD candidates in the initial screening. Therefore, of 502 putative iUPD genotypes in the CEU 1463 trio, 100 candidate sites (300 genotypes in the trio) were selected at random, and validated by capillary sequencing on the LCLs DNA. We used this data to estimate the accuracy of the genotype and to determine the threshold quality more efficiently for identification of the true iUPD genotype. Of the 300 validated genotypes, the correct and incorrect genotypes were 189 (63%) and 111 (37%), respectively, and true iUPD genotype was not confirmed (Supplementary Table 7). For more efficient screening, we focused on genotype quality (GQ), encoded as a Phred quality and read depth (DP) at genotype position. The 300 genotypes validated had a mean GQ of 71.13 (from a minimum of 1.61 to a maximum of 99.00) and a mean DP of 31.79 (from a minimum of 8.00 to a maximum of 75.00), respectively. Studying the relationship between GQ and accuracy of the genotypes with GQ10 or more, the correct genotype rate was 64.9% (189/291), 72.5% (182/251) with GQ40 or more, 91.0% (162/178) with GQ60 or more and 99.3% (150/151) with GQ80 or more. Thus, a higher GQ showed a higher reliability (Supplementary Fig. 4A). In contrast, increasing DP simply did not have much power to remove incorrect genotypes (Supplementary Fig. 4B). Furthermore, the majority of false positives for putative iUPD genotypes arose from an inaccuracy of genotyping in any one of the trio (81.1%, 90/111). Therefore, we required all genotypes in the trio with GQ40 or greater for identification of the true iUPD genotype. After filtering with a threshold GQ40, we identified 100 and 178 putative iUPD genotypes in the CEU 1463 and YRI Y117 trio, respectively (Fig. 2, Supplementary Tables 8 and 9).

3.4. Validation of the putative iUPD genotypes by capillary sequencing and qPCR

We attempted to validate these candidates by capillary sequencing. Of these, only 1 putative iUPD genotype (Validation ID C1383 and Y3887, respectively), in the CEU 1463 and YRI Y117 trio was confirmed as a true iUPD genotype (Fig. 2, Supplementary Tables 8 and 9, Supplementary Fig. 5A and B). Although iUPD candidates were not present in the known CNVs regions in the daughter, qPCR analysis with DNA from each trio was performed with primers C1383 and Y3887 to confirm the copy number on the putative iUPD loci. The results revealed a deletion

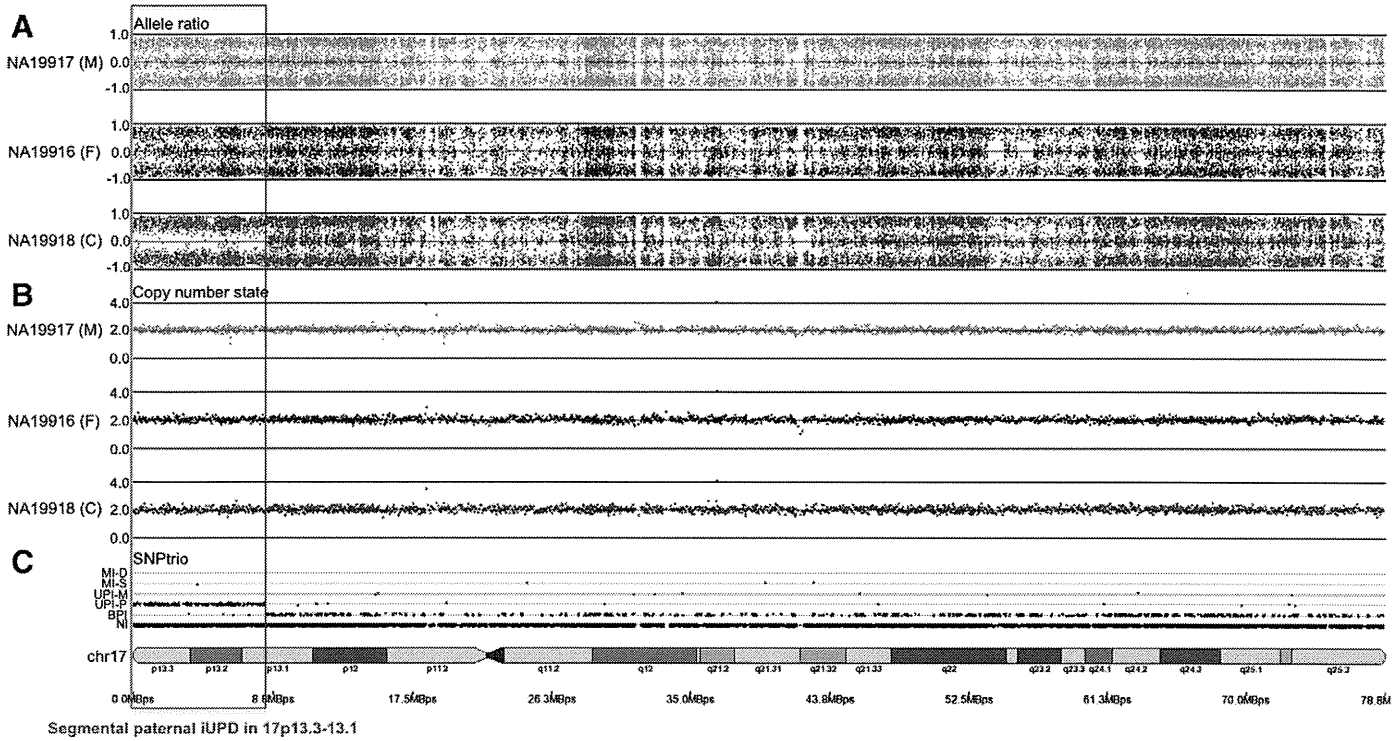

Fig. 1. Segmental paternal iUPD in HapMap ASW sample (NA19918). SNP6.0 data analyzed with PartekGS software shows the plots for the allele ratio, copy number state, and inheritance pattern by SNPtrio on chromosome 17 in HapMap ASW trio (FID 2431) (M, mother; F, father; C, child). (A) The allele ratio graph represents the genotypes for each individual single nucleotide polymorphism (SNP). Dots with a value of 1, −1, and 0 represent SNPs with AA, BB, and AB genotypes, respectively. (B) Plots represent chromosome copy number state (0.0–4.0). (C) SNPtrio displayed five classes of inheritance pattern. The five classes are 1) double Mendelian inconsistency (MI-D); 2) single Mendelian inconsistency (MI-S); 3) maternal uniparental inheritance (UPI-M); 4) paternal uniparental inheritance (UPI-P); 5) biparental inheritance (BPI). NI indicates not informative. The BPI plots represent the biparental inheritance SNPs, in which the parents have AA and BB calls and the child has an AB call. A red box indicates the segmental paternal iUPD locus.

on the C1383 locus in the daughter (NA12878) and mother (NA12892). Similarly, the results revealed a deletion on the Y3887 locus in the daughter (NA19240) and father (NA19239) (Supplementary Fig. 5C). In our investigation, we could not identify shorter segmental iUPD in the daughters from the two trios (Fig. 2).

3.5. Genes in identified segmental UPD regions in normal individuals

Finally, we identified one segmental paternal iUPD on 17p13.3-13.1 from 173 individuals. This segmental UPD region was included in the 233 RefSeq genes (Supplementary Table 10), but which are not "imprinted genes." According to the conventional concept, UPD has no practical impact on phenotypes with the exception of the disruption of imprinting and homozygosity for recessive mutations.

4. Discussion

At any stage of the life cycle, from gamete formation to fetal postnatal life, exposure to genotoxic stress may affect the genomic integrity and fate of the organism (Jaroudi and SenGupta, 2006; Vinson and Hales, 2002). In undifferentiated cells, such as the embryo and progenitor cells, mutations are propagated to multiple differentiated cell types

Table 2
Summary of alignment and base calling in two trios. AC+X: autosomal chromosome and X chromosome (exclude gap) = total length 2,706,959,439 bases (about 2.71 Gb).

Family	CEU 1463			YRI Y117		
Sample	NA12878	NA12891	NA12892	NA19240	NA19239	NA19238
Relation	Daughter	Father	Mother	Daughter	Father	Mother
Total bases (Gb)	102.24 Gb	100.89 Gb	85.68 Gb	108.25 Gb	84.03 Gb	71.56 Gb
Mapped bases (Gb)	99.63 Gb	97.25 Gb	80.2 Gb	104.25 Gb	79.94 Gb	65.24 Gb
Total reads	2,507,012,490	2,264,396,064	2,051,935,811	2,738,304,812	2,296,647,842	1,971,737,379
Mapped reads	2,443,207,477	2,189,660,230	1,952,966,402	2,632,175,898	2,184,252,515	1,796,606,841
Mean mapped depth	31.9	30.3	25.6	33.4	24.5	20.6
Accessible genome (Gb)	2.32 Gb	2.33 Gb	2.31 Gb	2.36 Gb	2.30 Gb	2.23 Gb
Accessible genome (% of AC+X)	85.61 (%)	85.98 (%)	85.24 (%)	87.08 (%)	84.87 (%)	82.29 (%)
Accessible genome with trio (Gb)	2.24 Gb			2.14 Gb		
Accessible genome with trio (Gb) (% of AC+X)	82.66 (%)			78.97 (%)		
SNPs (N)	2,854,439	2,846,437	2,785,908	3,602,569	3,395,713	3,090,355
SNPs in dbSNP132 (N)	2,838,282	2,831,464	2,773,304	3,576,164	3,371,626	3,070,416
SNPs in dbSNP132 (%)	99.43 (%)	99.47 (%)	99.55 (%)	99.27 (%)	99.29 (%)	99.35 (%)

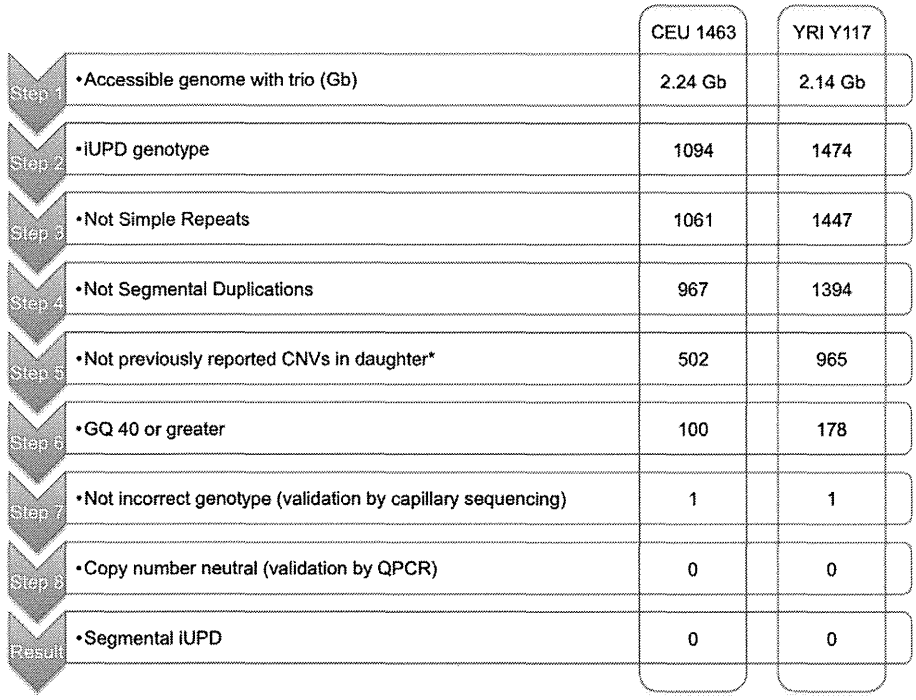

Fig. 2. Study design and summary of iUPD segment analysis using whole-genome sequencing (WGS) data of HapMap FID CEU 1463 and YRI Y117 trios, respectively. GQ, genotype quality; qPCR, quantitative polymerase chain reaction. *Previously reported CNV regions (Conrad et al., 2010; Kidd et al., 2008; McCarroll et al., 2008; Mills et al., 2011).

within the organism. Therefore, undifferentiated cells would require error-less repair mechanisms. HR would be a suitable repair mechanism for such cells, because intact homologous chromosomes are used as repair templates. Indeed, embryonic stem cells (ESCs) repair DSBs more frequently using the error-free HR pathway rather than the error-prone NHEJ (Tichy, 2011; Tichy and Stambrook, 2008). HR (also called gene conversion) can occur between sister chromatids, homologous chromosomes or homologous sequences on either the same chromatid or different chromosomes (Chen et al., 2007). Although the extent of genetic loss is minimal if HR results in a non-crossover gene conversion, crossover gene conversion leads to iUPD of the large region of the chromosome in daughter cells (Moynahan and Jasin, 1997, 2010; Stark and Jasin, 2003). The occurrence of inter-allelic HR causing human inherited disease is rare (Chen et al., 2007). To our knowledge, homozygous nonsense mutations due to inter-allelic HR have been reported in a patient with campomelic dysplasia (Y440X) in SRY-box 9 (SOX9) (Pop et al., 2005). This case indicates that inter-allelic HR in early stage embryogenesis can occur.

To assess the possibility that inter-allelic HR occurs in the human genome during the period between postzygotic cells and the early embryonic stage to maintain the higher fidelity of genomic integrity, we investigated the traits of iUPD genotypes using NGS data during the pilot phase 2 of the 1000 Genomes Project. However, we could not find direct evidence of segmental iUPD after the accurate reconfirmation process including capillary sequencing and qPCR. Some parts of the reference sequence are inaccessible because of high-copy repeats or segmental duplications. This is a limitation of the current NGS technology producing short sequence reads. Indeed, 20% of the reference genome was inaccessible in the trio project (Altshuler et al., 2010). From our data, the accessible genome per CEU and YRI trio set were 2.24 Gb and 2.14 Gb, respectively (Table 1). Because the total length of the human reference genome, including the gap was composed of about 3.08 Gb, 27.2% and 30.5% of data in CEU and YRI trio, respectively, were not analyzed in this study. Furthermore, the use of only two trios might be too small a scale and low-level mosaicism is often difficult to detect accurately. However, the data presented here provides evidence that segmental UPD during normal development could not be a constitutive event in order to maintain genomic integrity.

Constitutive UPD is very rare. Robinson (2000) determined that UPD for an average chromosome occurs in 1/80,000 births (0.00125%) and UPD for any chromosome can be expected in roughly 1/3,500 births (0.02857%), based on the frequency of UPD15. Liehr (2010) suggested that the rate of UPD in human population might be even lower than 1 in 5,000 or less. We studied 173 trios using genome-wide SNP array and WGS data using NGS, and identified one case with segmental iUPD. Segmental UPD for any chromosome can be expected in 1/173 births which equals a rate of 0.57803%. Based on the investigated autosomal chromosome pairs, we estimate the rate of segmental UPD to be one per 3806 chromosome pairs that equals a rate of 0.02627%. We found a higher frequency of UPD events than the previously reported frequency by Robinson and Liehr. These data imply the possibility of hidden segmental UPD in normal individuals. However, we found just only one UPD in 3806 chromosome pairs, we need analyze more trio samples and that would give the accurate rate of whole chromosomal and/or segmental UPD.

iUPD resulting from a somatic recombination can cause LOH. Somatic recombination leading to mosaic segmental UPD could occur in any individual and it is likely to be mosaic or in a heterogeneous cell population with increased cell division. In fact, the studies by Laurie et al. (2012) and Jacobs et al. (2012) found that detectable mosaic genomic variations including segmental UPD were rare (1%) in adults younger than 50 but that its prevalence increased to 2–3% in individuals older than 70. We detected 21 LTAs over 200 kb in the process of UPD screening using SNP microarray (Table 1 and supplementary Figs. 2 and 3). These genomic alterations may reflect that CNVs or segmental UPD result from somatic recombination in restricted soma (for example, in hematopoietic cells) or during cell culture, as with aging. Although most sample data analyzed here was derived from DNA of LCLs (170 trios from HapMap), we suggest that segmental UPD occurring in early developmental stages in individuals in the general population can be detected. However, we cannot totally negate the possibility that one

segmental UPD identified in this study arose during passage in the artificial culture.

Studies of UPD have only been performed in cases with relevant phenotypic features and included only a few markers. These facts suggest that researchers may overlook UPD in normal development and miss shorter segmental UPD, because UPD of many chromosomal regions results in no obvious abnormalities (Kotzot and Utermann, 2005; Robinson, 2000). In addition, lethal genotypes due to UPD during early embryonic development would be undetectable. We suggest that trio genome analysis with enhanced sequence accuracy could provide new findings for the risk of recessive disorders, because one mutant allele from one parent can be transmitted to a child and result in a homozygous state due to iUPD. To the best of our knowledge, this is the first systematic study over whole chromosomal and segmental UPD in the human genome without abnormal phenotype using familial trios.

5. Conclusions

The current study assessed the presence of whole chromosome and segmental UPD in general populations using genome-wide SNP microarray and WGS data. We provided evidence that segmental UPD in normal development is not a constitutive event in order to maintain genomic integrity. Although we identified one obvious segmental paternal iUPD in one HapMap sample, we could not find direct evidence of shorter segmental iUPD. This suggested three possibilities, 1) human cells repress the usage of inter-allelic homologous sequences as a template for HR, even at the early embryonic stage, 2) shorter iUPD segments are unidentifiable because of absent informative markers within the limited short segment, 3) UPD could be present in inaccessible genome regions when using current NGS with short reads. Investigation of segmental UPD in general populations will help to expand our general understanding of normal development in humans.

Conflict of interest

None of the authors of this paper declares a conflict of interest.

Acknowledgements

We express our gratitude to the families for their participation in this research and the anonymous HapMap families for contributing samples for research. We also thank Ms. Chisa Hayashida for technical assistance. K.Y. was supported by a Grant-in-Aid for Challenging Exploratory Research (No. 22659071) from the Japan Society for the Promotion of Science.

Appendix A. Supplementary data

Supplementary data to this article can be found online at http://dx.doi.org/10.1016/j.gene.2012.10.035.

References

Altshuler, D., et al., 2010. A map of human genome variation from population-scale sequencing. Nature 467, 1061–1073.
Altug-Teber, O., et al., 2005. A rapid microarray based whole genome analysis for detection of uniparental disomy. Hum. Mutat. 26, 153–159.
Amor, D.J., Halliday, J., 2008. A review of known imprinting syndromes and their association with assisted reproduction technologies. Hum. Reprod. 23, 2826–2834.
Baumer, A., et al., 2001. A novel MSP/DHPLC method for the investigation of the methylation status of imprinted genes enables the molecular detection of low cell mosaicisms. Hum. Mutat. 17, 423–430.
Chen, J.M., et al., 2007. Gene conversion: mechanisms, evolution and human disease. Nat. Rev. Genet. 8, 762–775.
Conrad, D.F., et al., 2010. Origins and functional impact of copy number variation in the human genome. Nature 464, 704–712.
Conrad, D.F., et al., 2011. Variation in genome-wide mutation rates within and between human families. Nat. Genet. 43, 712–714.
D'haene, B., et al., 2010. Accurate and objective copy number profiling using real-time quantitative PCR. Methods 50, 262–270.
DePristo, M.A., et al., 2011. A framework for variation discovery and genotyping using next-generation DNA sequencing data. Nat. Genet. 43, 491–498.
Engel, E., 1980. A new genetic concept: uniparental disomy and its potential effect, isodisomy. Am. J. Med. Genet. 6, 137–143.
Hannula, K., et al., 2000. A narrow segment of maternal uniparental disomy of chromosome 7q31-qter in Silver-Russell syndrome delimits a candidate gene region. Am. J. Hum. Genet. 68, 247–253.
Hartlerode, A.J., Scully, R., 2009. Mechanisms of double-strand break repair in somatic mammalian cells. Biochem. J. 423, 157–168.
Jacobs, K.B., et al., 2012. Detectable clonal mosaicism and its relationship to aging and cancer. Nat. Genet. 44, 651–658.
Jaroudi, S., SenGupta, S., 2006. DNA repair in mammalian embryos. Mutat. Res. 635, 53–77.
Kidd, J.M., et al., 2008. Mapping and sequencing of structural variation from eight human genomes. Nature 453, 56–64.
Kotzot, D., 2001. Complex and segmental uniparental disomy (UPD): review and lessons from rare chromosomal complements. J. Med. Genet. 38, 497–507.
Kotzot, D., 2008. Complex and segmental uniparental disomy updated. J. Med. Genet. 45, 545–556.
Kotzot, D., Utermann, G., 2005. Uniparental disomy (UPD) other than 15: phenotypes and bibliography updated. Am. J. Med. Genet. A 136, 287–305.
Laurie, C.C., et al., 2012. Detectable clonal mosaicism from birth to old age and its relationship to cancer. Nat. Genet. 44, 642–650.
Liehr, T., 2010. Cytogenetic contribution to uniparental disomy (UPD). Mol. Cytogenet. 3, 8.
McCarroll, S.A., et al., 2008. Integrated detection and population-genetic analysis of SNPs and copy number variation. Nat. Genet. 40, 1166–1174.
McKenna, A., et al., 2010. The Genome Analysis Toolkit: a MapReduce framework for analyzing next-generation DNA sequencing data. Genome Res. 20, 1297–1303.
Mills, R.E., et al., 2011. Mapping copy number variation by population-scale genome sequencing. Nature 470, 59–65.
Moynahan, M.E., Jasin, M., 1997. Loss of heterozygosity induced by a chromosomal double-strand break. Proc. Natl. Acad. Sci. U. S. A. 94, 8988–8993.
Moynahan, M.E., Jasin, M., 2010. Mitotic homologous recombination maintains genomic stability and suppresses tumorigenesis. Nat. Rev. Mol. Cell Biol. 11, 196–207.
Pérez, B., et al., 2011. Segmental uniparental disomy leading to homozygosity for a pathogenic mutation in three recessive metabolic diseases. Mol. Genet. Metab. 105, 270–271.
Pop, R., et al., 2005. A homozygous nonsense mutation in SOX9 in the dominant disorder campomelic dysplasia: a case of mitotic gene conversion. Hum. Genet. 117, 43–53.
Quinlan, A.R., Hall, I.M., 2010. BEDTools: a flexible suite of utilities for comparing genomic features. Bioinformatics 26, 841–842.
Redon, R., et al., 2006. Global variation in copy number in the human genome. Nature 444, 444–454.
Robinson, W.P., 2000. Mechanisms leading to uniparental disomy and their clinical consequences. Bioessays 22, 452–459.
Rodríguez-Santiago, B., et al., 2010. Mosaic uniparental disomies and aneuploidies as large structural variants of the human genome. Am. J. Hum. Genet. 87, 129–138.
Sonoda, E., et al., 2006. Differential usage of non-homologous end-joining and homologous recombination in double strand break repair. DNA Repair (Amst) 5, 1021–1029.
Stark, J.M., Jasin, M., 2003. Extensive loss of heterozygosity is suppressed during homologous repair of chromosomal breaks. Mol. Cell. Biol. 23, 733–743.
Tichy, E.D., 2011. Mechanisms maintaining genomic integrity in embryonic stem cells and induced pluripotent stem cells. Exp. Biol. Med. (Maywood) 236, 987–996.
Tichy, E.D., Stambrook, P.J., 2008. DNA repair in murine embryonic stem cells and differentiated cells. Exp. Cell Res. 314, 1929–1936.
Ting, J.C., et al., 2007. Visualization of uniparental inheritance, Mendelian inconsistencies, deletions, and parent of origin effects in single nucleotide polymorphism trio data with SNPtrio. Hum. Mutat. 28, 1225–1235.
Tsai, M.F., et al., 2007. PrimerZ: streamlined primer design for promoters, exons and human SNPs. Nucleic Acids Res. 35 (Web Server issue), W63–5.
Untergasser, A., et al., 2007. Primer3Plus, an enhanced web interface to Primer3. Nucleic Acids Res. 35 (Web Server issue), W71–4.
Vinson, R.K., Hales, B.F., 2002. DNA repair during organogenesis. Mutat. Res. 509, 79–91.
Wang, K., et al., 2010. ANNOVAR: functional annotation of genetic variants from high-throughput sequencing data. Nucleic Acids Res. 38, e164.
Wyman, C., Kanaar, R., 2006. DNA double-strand break repair: all's well that ends well. Annu. Rev. Genet. 40, 363–383.

Web references

1000 Genomes Project pilot 2 data, A. ftp://ftp-trace.ncbi.nih.gov/1000genomes/ftp/pilot_data/data/.
1000 Genomes Project, a. http://www.1000genomes.org/.
Best Practice Variant Detection with the GATK v2, a. http://www.broadinstitute.org/gsa/wiki/index.php/Best_Practice_Variant_Detection_with_the_GATK_v2.

Coriell Institute, a. http://ccr.coriell.org/sections/collections/NHGRI/?SsId=11.
Geneimprint, a. http://www.geneimprint.com/site/genes-by-species.Homo+sapiens.imprinted-All.
HapMap 3 raw data, . ftp://ftp.ncbi.nlm.nih.gov/hapmap/raw_data/hapmap3_affy6.0/.
Liehr, T., 2012. Cases with uniparental disomy. http://www.fish.uniklinikum-jena.de/UPD.html.
Picard (version 1.38), a. http://picard.sourceforge.net/.
Primer3Plus, a. http://www.bioinformatics.nl/cgi-bin/primer3plus/primer3plus.cgi.
PrimerZ, a. http://genepipe.ngc.sinica.edu.tw/primerz/beginDesign.do.
The National Center for Biotechnology Information (NCBI), a. http://www.ncbi.nlm.nih.gov/.
The University of California Santa Cruz (UCSC), a. http://genome.ucsc.edu/.

RESEARCH ARTICLE

AMERICAN JOURNAL OF medical genetics PART A

Clinical Correlations of Mutations Affecting Six Components of the SWI/SNF Complex: Detailed Description of 21 Patients and a Review of the Literature

Tomoki Kosho,[1]* Nobuhiko Okamoto,[2] Hirofumi Ohashi,[3] Yoshinori Tsurusaki,[4] Yoko Imai,[5] Yumiko Hibi-Ko,[5] Hiroshi Kawame,[6,7] Tomomi Homma,[8] Saori Tanabe,[9] Mitsuhiro Kato,[10] Yoko Hiraki,[11] Takanori Yamagata,[12] Shoji Yano,[13] Satoru Sakazume,[14] Takuma Ishii,[14,15] Toshiro Nagai,[14] Tohru Ohta,[16] Norio Niikawa,[16] Seiji Mizuno,[17] Tadashi Kaname,[18] Kenji Naritomi,[18] Yoko Narumi,[1] Keiko Wakui,[1] Yoshimitsu Fukushima,[1] Satoko Miyatake,[4] Takeshi Mizuguchi,[4] Hirotomo Saitsu,[4] Noriko Miyake,[4] and Naomichi Matsumoto[4]**

[1]Department of Medical Genetics, Shinshu University School of Medicine, Matsumoto, Japan

[2]Department of Medical Genetics, Osaka Medical Center and Research Institute for Maternal and Child Health, Izumi, Japan

[3]Division of Medical Genetics, Saitama Children's Medical Center, Saitama, Japan

[4]Department of Human Genetics, Yokohama City University Graduate School of Medicine, Yokohama, Japan

[5]Division of Pediatrics, Japanese Red Cross Medical Center, Tokyo, Japan

[6]Department of Genetic Counseling, Graduate School of Humanities and Sciences, Ochanomizu University, Tokyo, Japan

[7]Division of Medical Genetics, Nagano Children's Hospital, Azumino, Japan

[8]Division of Pediatrics, Yamagata Prefectural Shinjo Hospital, Shinjo, Japan

[9]Division of Pediatrics, Yamagata Prefectural and Sakata Municipal Hospital Organization Nihon-Kai General Hospital, Sakata, Japan

[10]Department of Pediatrics, Yamagata University Faculty of Medicine, Yamagata, Japan

[11]Hiroshima Municipal Center for Child Health and Development, Hiroshima, Japan

[12]Department of Pediatrics, Jichi Medical University, Shimotsuke, Japan

[13]Genetics Division, Department of Pediatrics, LAC + USC Medical Center, Keck School of Medicine, University of Southern California, Los Angeles, California,

[14]Department of Pediatrics, Dokkyo Medical University Koshigaya Hospital, Koshigaya, Japan

[15]Nakagawa-No-Sato (Hospital for the Disabled), Matsubushi, Japan

[16]Research Institute of Personalized Health Sciences, Health Sciences University of Hokkaido, Tobetsu, Japan

Conflict of Interest: The authors have no conflict of interest to declare.

Grant sponsor: Ministry of Health, Labour and Welfare; Grant sponsor: Japan Science and Technology Agency; Grant sponsor: Strategic Research Program for Brain Sciences; Grant sponsor: Grant-in-Aid for Scientific Research on Innovative Areas (Transcription cycle) from the Ministry of Education, Culture, Sports, Science and Technology of Japan; Grant sponsor: Grant-in-Aid for Scientific Research from the Japan Society for the Promotion of Science; Grant sponsor: Grant-in-Aid for Young Scientists from the Japan Society for the Promotion of Science; Grant sponsor: Grant for 2012 Strategic Research Promotion of Yokohama City University; Grant sponsor: Research Grants from the Japan Epilepsy Research Foundation; Grant sponsor: Takeda Science Foundation.

*Correspondence to:
Dr. Tomoki Kosho, M.D., Department of Medical Genetics, Shinshu University School of Medicine, 3-1-1 Asahi, Matsumoto, Nagano 390-8621, Japan. E-mail: ktomoki@shinshuu.ac.jp

**Correspondence to:
Naomichi Matsumoto, M.D., Ph.D., Department of Human Genetics, Yokohama City Graduate School of Medicine, 3-9 Fukuura, Kanazawa-Ku, Yokohama 236-0004, Japan. E-mail: naomat@yokohama-cu.ac.jp

Article first published online in Wiley Online Library (wileyonlinelibrary.com): 1 May 2013
DOI 10.1002/ajmg.a.35933

[17]Department of Pediatrics, Central Hospital, Aichi Human Service Center, Kasugai, Japan
[18]Department of Medical Genetics, Faculty of Medicine, University of the Ryukyus, Nishihara, Japan

Manuscript Received: 31 August 2012; Manuscript Accepted: 11 February 2013

Mutations in the components of the SWItch/sucrose nonfermentable (SWI/SNF)-like chromatin remodeling complex have recently been reported to cause Coffin–Siris syndrome (CSS), Nicolaides–Baraitser syndrome (NCBRS), and *ARID1B*-related intellectual disability (ID) syndrome. We detail here the genotype-phenotype correlations for 85 previously published and one additional patient with mutations in the SWI/SNF complex: four with *SMARCB1* mutations, seven with *SMARCA4* mutations, 37 with *SMARCA2* mutations, one with an *SMARCE1* mutation, three with *ARID1A* mutations, and 33 with *ARID1B* mutations. The mutations were associated with syndromic ID and speech impairment (severe/profound in *SMARCB1*, *SMARCE1*, and *ARID1A* mutations; variable in *SMARCA4*, *SMARCA2*, and *ARID1B* mutations), which was frequently accompanied by agenesis or hypoplasia of the corpus callosum. *SMARCB1* mutations caused "classical" CSS with typical facial "coarseness" and significant digital/nail hypoplasia. *SMARCA4* mutations caused CSS without typical facial coarseness and with significant digital/nail hypoplasia. *SMARCA2* mutations caused NCBRS, typically with short stature, sparse hair, a thin vermillion of the upper lip, an everted lower lip and prominent finger joints. A *SMARCE1* mutation caused CSS without typical facial coarseness and with significant digital/nail hypoplasia. *ARID1A* mutations caused the most severe CSS with severe physical complications. *ARID1B* mutations caused CSS without typical facial coarseness and with mild digital/nail hypoplasia, or caused syndromic ID. Because of the common underlying mechanism and overlapping clinical features, we propose that these conditions be referred to collectively as "SWI/SNF-related ID syndromes". © 2013 Wiley Periodicals, Inc.

Key words: Coffin–Siris syndrome; SWI/SNF complex; *SMARCB1*; *SMARCA4*; *SMARCA2*; *SMARCE1*; *ARID1A*; *ARID1B*; Nicolaides–Baraitser syndrome; intellectual disability (ID)

How to Cite this Article:
Kosho T, Okamoto N, Ohashi H, Tsurusaki Y, Imai Y, Hibi-Ko Y, Kawame H, Homma T, Tanabe S, Kato M, Hiraki Y, Yamagata T, Yano S, Sakazume S, Ishii T, Nagai T, Ohta T, Niikawa N, Mizuno S, Kaname T, Naritomi K, Narumi Y, Wakui K, Fukushima Y, Miyatake S, Mizuguchi T, Saitsu H, Miyake N, Matsumoto N. 2013. Clinical correlations of mutations affecting six components of the SWI/SNF complex: detailed description of 21 patients and a review of the literature.
Am J Med Genet Part A 161A:1221–1237.

INTRODUCTION

Coffin–Siris syndrome (CSS; OMIM 135900) was first described by Coffin and Siris [1970]. It is a rare congenital anomaly syndrome characterized by developmental delay or intellectual disability (ID), coarse facial appearance, feeding difficulties, frequent infections, and hypoplastic-to-absent fifth fingernails and fifth distal phalanges [Devy and Baraitser, 1991; Fleck et al., 2001; Schrier et al., 2012]. We recently reported on mutations in six genes encoding components of the SWItch/sucrose nonfermentable (SWI/SNF)-like chromatin remodeling complex in 20 of 23 patients clinically diagnosed with CSS: *SMARCB1* in four patients, *SMARCA4* in six, *SMARCA2* in one, *SMARCE1* in one, *ARID1A* in three, and *ARID1B* in five [Tsurusaki et al., 2012]. In the same journal issue, truncating mutations in *ARID1B* were reported in three patients with CSS and microdeletions encompassing *ARID1B* were reported in three patients with ID and remnants of CSS [Santen et al., 2012]. Furthermore, missense mutations of *SMARCA2* were reported in 36 patients with Nicolaides–Baraitser syndrome (NCBRS; OMIM#601358) [van Houdt et al., 2012]. NCBRS was first described by Nicolaides and Baraitser [1993] and it is a recently delineated condition characterized by severe ID with absent/limited speech, seizures, short stature, sparse hair, typical facial characteristics, brachydactyly, prominent finger joints, and broad distal phalanges; the main differential diagnosis is CSS [Sousa et al., 2009]. *ARID1B* has also been reported to be a cause of ID. Nagamani et al. [2009] reported four patients with interstitial deletion of 6q25.2–q25.3 including *ARID1B*, all of whom manifested microcephaly, developmental delay, facial characteristics, and hearing impairment, and two of whom had agenesis of the corpus callosum. Halgren et al. [2012] reported eight patients with haploinsufficiency of *ARID1B* (de novo chromosomal translocation involving *ARID1B* in one, intragenic deletions in three, and microdeletion including *ARID1B* in four), who manifested agenesis or hypoplasia of the corpus callosum, ID with speech impairment, and autism. Hoyer et al. [2012] very recently concluded that haploinsufficiency of *ARID1B* is a relatively frequent cause of moderate-to-severe ID from their findings that 0.9% (8/887) of patients with unexplained ID had truncating mutations in the gene. Michelson et al. [2012] also very recently reported a patient with an interstitial 1.19 Mb deletion of 6q25.2 including *ARID1B* and *ZDHHC14*, who manifested global developmental delay, facial characteristics, dysgenesis of the corpus callosum, limb anomalies, and genital hypoplasia.

To delineate the clinical consequences of mutations affecting components of the SWI/SNF complex (CSS, NBS, and *ARID1B*-related ID syndrome), we report the individual clinical information for 20 previously reported patients [Tsurusaki et al., 2012] as well as an additional patient with an *SMARCA4* mutation. Furthermore, we create a comprehensive list of all reported patients (including our series) with mutations affecting components of the SWI/SNF complex (Tables Ia–Ic), which will be helpful when discussing similarities and differences among these conditions.

CLINICAL REPORTS

SMARCB1 Mutations

SMARCB1-1 (Subject 4 [Tsurusaki et al., 2012]; Fig. 1a–i): She was born at 42 weeks of gestation after an uncomplicated prenatal period. Her birth weight was 3,008 g (−0.5 SD). She had: cleft palate with exudative otitis media; congenital dislocation of the right hip; pectus excavatum; sucking/feeding difficulty. She underwent surgical correction of cleft palate and insertion of ventilation tubes at age 2 6/12 years. Hearing aids were required for bilateral, severe, mixed hearing impairment with a threshold of 80–90 dB. At age 4 years, she developed tonic seizures, which were treated with carbamazepine. Scoliosis, found at age 2 years, progressed with a Cobb angle of ≈150°. She showed hypotonia and motor development was severely delayed: she raised her head at age 1 8/12 years, sat alone at 2 3/12 years, and walked independently at 7 years. From ages 12 to 18 years, she vomited frequently and had recurrent infections. She had multiple dental caries, treated under general anesthesia at age 16 years. At age 21 years, she weighs 30 kg (−3.4 SD), her height is 112.5 cm (−8.4 SD), and her occipitofrontal circumference (OFC) is 51.2 cm (−2.9 SD). She understands simple commands in daily life, expresses herself with gestures, and likes to play portable personal computer games, but speaks no words. She has serious behavioral problems such as impulsiveness, hyperactivity, and self-injurious behaviors (including skin picking). She becomes exhausted easily.

SMARCB1-2 (Subject 11 [Tsurusaki et al., 2012]): Her prenatal period was complicated by intrauterine growth retardation. She was born at 38 weeks of gestation. Her birth weight was 2,088 g (−1.8 SD), length was 42 cm (−2.9 SD), and OFC was 33 cm (0 SD). She had a small ventricular septal defect (VSD). Diaphragmatic hernia was corrected surgically at age 5 months. She had sucking/feeding difficulties. She showed hypotonia and motor development was severely retarded: she rolled over at age 3 years. Generalized seizures developed and were controlled with valproic acid. Magnetic resonance imaging (MRI) of the brain showed cerebellar hypoplasia and Dandy–Walker malformation. She had visual impairment that was corrected with spectacles; hearing impairment with a threshold of 60 dB in the right ear and 50 dB in the left ear was noted. At age 7 years, her weight is 12 kg (−3.1 SD) and height is 105 cm (−2.7 SD). She sits for several seconds with her hands, distinguishes her family members from others, and smiles when called by her name. She has visual and hearing impairment.

SMARCB1-3 (Subject 21 [Tsurusaki et al., 2012]; Fig. 1j–p): Her prenatal period was complicated by intrauterine growth retardation and oligohydramnios. She was born at 38 weeks of gestation, followed by resuscitation through endotracheal intubation. Her birth weight was 1,746 g (−2.6 SD). Surfactant treatment was undertaken for pulmonary hemorrhage. She had micrognathia, exotropia, and a dark complexion. She suffered from complex partial seizures. She sucked poorly and then had feeding difficulty associated with gastroesophageal reflux (GER), which required gastrostomy. She showed hypotonia with severe delay in motor development. A hypoplastic corpus callosum was observed. At age 7 years, she weighs 12 kg (−3.0 SD), has a height of 97 cm (−4.5 SD), and an OFC of 44 cm (−5.1 SD). She is unable to sit alone, and moves by rolling over. She cannot communicate with others or speak any words, but smiles when she appears to be happy.

SMARCB1-4 (Subject 22 [Tsurusaki et al., 2012]): He was born at 37 weeks of gestation. His birth weight was 2,784 g (+0.2 SD). He was admitted to hospital as a newborn for treatment of transient tachypnea. He had pyloric stenosis that was corrected surgically. He sucked poorly and then had feeding difficulties associated with GER, requiring gavage-feeding and resulting in failure to thrive. He showed hypotonia and motor development was severely delayed. MRI of the brain showed hypoplasia of the corpus callosum. He suffered from recurrent respiratory tract infections. At age 2 years, he weighed 9.7 kg (−2.3 SD), his height was 83.4 cm (−2.2 SD), and had an OFC of 43 cm (−3.3 SD). At age 3 years, he rolls over, but cannot sit alone or speak words.

SMARCA4 Mutations

SMARCA4-1 (Subject 9 [Tsurusaki et al., 2012]; Fig. 2a–c): He was born at 39 weeks of gestation. His birth weight was 2,880 g. Sucking or feeding difficulties were not reported, but abdominal distension occurred in infancy and constipation was frequent in childhood. Possible seizures developed once at age 1 2/12 years with unconsciousness but without electrocardiographic abnormalities. The submucosal cleft palate was corrected surgically at age 1 6/12 years. Congenital torticollis with vestigial (right) and shortened (left) cleidomastoid muscles was corrected surgically. His right chest was funnel-shaped with a hypoplastic right pectoral major muscle. Exudative otitis media in the left ear was recurrent. He showed hypotonia in his infancy and motor development was mildly delayed: he raised his head at age 4 months, sat alone at 10 months, crawled at 11 months, and stood alone at 1 3/12 years. His hair has been bristly and gray-streaked since childhood. His upper teeth were misaligned. At age 18 years, his height is 159 cm (−1.8 SD) and OFC is 53 cm (−2.3 SD). He can walk independently, talk (albeit with a stutter), and understand almost everything necessary for daily life. He has myopia and mild astigmatism which are corrected with spectacles. He has nocturnal enuresis which he finds hard to control.

SMARCA4-2 (Subject 7 [Tsurusaki et al., 2012]; Fig. 2d–g): His prenatal period was complicated by intrauterine growth retardation. He was born at 40 weeks of gestation. His birth weight was 2,250 g (−2.2 SD). He showed respiratory insufficiency and had sucking/feeding difficulties associated with laryngomalacia. He had bilateral ptosis, myopia, lacrimal duct stenosis, bilateral sensorineural hearing loss, and ankyloglossia. He showed hypotonia and motor development was severely delayed: he raised his head in late infancy, sat alone at age 2 years, and walked independently at 6 years. At age 20 years, he weighs 60 kg (−0.2 SD), has a height of

TABLE IA. Clinical Features of Patients With Mutations in the Components of SWI/SNF Complex

Gene	*SMARCB1*				*SMARCA4*						
Patient (subject no. in the previous report§)	1 (4)	2 (11)	3 (21)	4 (22)	1 (9)	2 (7)	3 (5)	4 (16)	5 (25)	6 (17)	7
Age at publication (years of age)	21	7	7	2	18	20	9	11	16	4	8
Sex	F	F	F	M	M	M	M	M	F	M	F
Mutation	p.Lys364del	p.Arg377His	p.Lys364del	p.Lys364del	p.Lys546del	p.Thr859Met	p.Arg885Cys	p.Leu921Phe	p.Met1011Thr	p.Arg1157Gly	p.Arg885His
Growth											
Prenatal growth (birth weight/length)#	−0.5/?	−1.8/−2.9	−2.6/?	+0.2/?	–	−2.2/?	−1.2/−0.9	−1.7/−1.6	−1.0/−1.9	−1.1/−2.3	−2.6/−2.7
Postnatal growth (weight/height)†	−3.4/−8.4	−3.1/−2.7	−3.0/−4.5	−2.3/−2.2	?/−1.8	−0.2/−2.6	−1.5/−3.2	−1.8/−3.1	−1.9/−1.9	−3.0/−3.4	−1.9/−1.8
Psychomotor											
Developmental delay/intellectual disability‡	Severe	Severe	Severe	Severe	Mild	Severe	Severe	Severe	Severe	Severe	Moderate
Speech delay	NW	NW	NW	NW	Mild	SW	NW	NW	SC	NW	Mild
Seizures	+	+	–	–	+	–	–	+	–	–	–
Hypotonia	+	+	+	+	+	+	+	–	+	–	+
Autistic features/behavioral abnormalities	HA,Im,SH		–			HA, Im	ASD (HA, HS, Ob, SH)	–	RB		HA
Microcephaly (≤2 SD) (SD score)	+(−2.9)	–	+(−5.1)	+(−3.3)	+(−2.3)	+(−3.8)	+(−3.6)	+(−2.9)	+(−2.3)	+(−2.7)	+(−3.0)
Brain anomaly		CH,DW	HCC	HCC			HCC,HCV			HCC	–
Craniofacial											
Sparse hair	+	+	+	+	–	+	–	+	–	+	–
Thick eyebrows	+	+	+	+	+	+	+	+	+	+	+
Thick eyelashes	+	+	+	+	+	+	+	+	+	+	+
Ptosis	–	+	+	+	+	+	+	+	–	+	+
Abnormal ears	+	+	+	+	–	+	+	+	+	+	–
Nasal bridge	Broad	Broad	Broad	Broad	Narrow	Narrow	Normal	Flat	Flat	Flat	Flat
Thick, anteverted alae nasi	–	–	–	+	–	–	–	–	–	–	–
Wide mouth	+	+	+	+	–	–	+	–	+	–	+
Philtrum	Broad		Long	Long	Short	Short	Short		Short		Short
Upper lip vermilion feature	Thin		Thin	Thick	Everted	Everted	Everted	Thin	Everted	–	
Thick lower lip vermilion	+	+	+	+	–	+	+	+	+	+	+
Palatal abnormality	C	C	H	H	SMCP	H	C	H	H	C	H
Skeletal–limb											
Hypoplastic/absent fifth finger/toe	Fi/T	Fi/T	Fi/T	Fi/T	Fi	Fi/T	T	Fi/T	Fi/T	Fi/T	T
Hypoplastic/absent nail (fifth finger/toe)	Fi/T	+	Fi/T	Fi/T	Fi	Fi/T	T	Fi/T	Fi/T	Fi/T	T
Hypoplastic/absent nail (other fingers/toes)	Fi/T		Fi/T	Fi/T		Fi/T	T	Fi/T	Fi/T	Fi/T	–
Prominent interphalangeal joints	+		–	–	–	+	–	–	+	–	–
Prominent distal phalanges	+	+	–	–	+	+	+	+	+	–	
Scoliosis/spinal abnormalities	+		+	+	–	+	–	–	–	–	–
Joint laxity		–	+	+	–	+	+	–	+	–	+
Others											
Hirsutism	+	–	+	+	+	+	+	+	+	+	+
Congenital heart defects	–	VSD	–	+	–	–	–	VSD, PDA	–	MA, PA, SRV, AtSD, PDA	+
Genitourinary defects	–			+	–		Cr	–	–	Cr	–
Gastrointestinal abnormalities	–	–	GER	PS		GOO	Co	DU	Co	GER	GER
Inguinal (I)/umbilical (U) hernia	–	–	I	I	–	I	–	I	–	Om	I/U
Sucking difficulty	+	+	+	+	–	+	+	+	+	+	+
Feeding difficulty	+	+	+	+	–	+	+	+	+	+	+
Frequent vomiting	+										+
Hearing impairment	+	+	+		–	+	+	–	+	–	–
Visual impairment		+	+		+	+	+	+	+	–	–
Recurrent infections	+	–	+	+	–	+	–	+	+	+	+

+, present; −, absent; blank, data not available; §, Tsurusaki et al. [2013]; #, SD score; †, SD acore; ‡, at latest assessment; ASD, autism spectrum disorder; AtSD, atrial septal defect; C, cleft palate; CH, cerebellar hypoplasia; Co, constipation; Cr, cryptorchidism; DU, duodenal ulcer; DW, Dandy-Walker malformation; F, female; Fi, finger; GER, gastroesophageal reflux; GOO, gastric outlet obstruction; H, high palate; HA, hyperactivity; HCC, hypoplastic corpus callosum; HCV, hypoplastic cerebellar vermis; HS, hypersensitivity; I, inguinal; Im, impulsiveness; M, male; MA, mitral atresia; NW, no words; Ob, obsession; Om, omphalocele; PA, pulmonary atresia; PDA, patent ductus arteriosus; PS, pyloric stenosis; RB, repetitive behavior; SC, simple conversation; SH, self-harming behavior; SMCP, submucosal cleft palate; SRV, single right ventricle; SW, several words; T, toe; VSD, ventricular septal defect

TABLE IB. Clinical Features of Patients With Mutations in the Components of SWI/SNF Complex

Gene	*SMARCA2*		*SMARCE1*	*ARID1A*			*ARID1B*			
Patient (subject no. in the previous report§)	1 (19)	NCBRS(n = 36)	1 (24)	1 (3)	2 (6)	3 (8)	1 (1)	2 (15)	3 (23)	4 (10)
Age at publication (years of age)	8	2 3/12–32	14	2	1	10	13	?	10	11
Sex	M	21M,15F	F	M	M	M	M	M	F	M
Mutation	Partial deletion [van Houdt et al., 2012]	Missense	p.Tyr73Cys	p.Ser11Alafs*91	p.Gln920*	p.Arg1335*	p.Ile560Glyfs*89	p.Gln635*	p.Arg1102*	p.Asp1878Metfs*96
Growth										
Prenatal growth (birth weight/length)#	−2.6/−3.1	10/34	−2.3/?	−1.0/−1.4	−0.6/−1.1	–	−0.9/+0.4	−1.2/−1.2	+0.5/−1.7	−1.0/−1.1
Postnatal growth (weight/height)†	−2.1/−3.8	19/36	−4.4/−6.8	−6.2/−8.9	−5.5/−8.2	50th/3rd	−0.5/−1.4	−1.1/−1.1	+1.5/−1.3	−0.5/−2.4
Psychomotor										
Developmental delay/intellectual disability‡	Moderate	3Mild,9Moderate, 24Severe	Severe	Severe	Severe	Severe	Moderate	Severe	Mild	Mild
Speech delay	NW	13/33NW	NW	NW	NW	NW	NW	NW	Mild	Mild
Seizures	+	22/35	+	−	−		−	+	+	−
Hypotonia	+		+	+	+	−	+	+	+	+
Autistic features/behavioral abnormalities	−					HA	ASD (HA, Im, O)	ASD (Im)	−	−
Microcephaly [≦2 SD] (SD score)	+(−3.3)	19/34	+(−6.7)	+(−3.7)	+(−3.1)	−(50th)	−(+0.7)	−(−1.4)	−(+1.8)	−(−1.1)
Brain anomaly				ACC, CH,DW	ACC	HCC	−		ACC, Colp	−
Craniofacial										
Sparse hair	−	35/36	+	+	+	+	+	−	−	+
Thick eyebrows	+		+	+	+	+	+	+	+	+
Thick eyelashes	+	23/35	+	+	+	+	+	+	+	+
Ptosis	+		+	−	−	−	−	−	−	−
Abnormal ears	+		+	+	+	+	+	+	−	+
Nasal bridge	Broad	22/36Narrow	Narrow	Broad	Broad		Broad	Broad	Broad	Broad
Thick, anteverted alae nasi	+	32/36	−		−	−	−	+	−	−
Wide mouth	+	34/36	+	+	+	+	+	+	−	+
Philtrum	Broad	31/36Broad, 29/36Long	Long	Short	Broad	Long	Broad	Broad	Long	Long
Upper lip vermilion feature		27/36Thin			Everted		Thin	Thick	Thin	Thin
Thick lower lip vermilion	+	32/36	+	+	+	+	−	+	+	+
Palatal abnormality	−		C	C	C	H	H	H	H	H
Skeletal—limb										
Hypoplastic/absent fifth finger/toe	−		Fi/T		Fi/T	Fi/T	Fi/T	Fi/T	Fi	Fi/T
Hypoplastic/absent nail (fifth finger/toe)	−		Fi/T	+	Fi/T	Fi/T	Fi/T	T	Fi	Fi/T
Hypoplastic/absent nail (other fingers/toes)	−		Fi/T	Fi/T		Fi/T	Fi/T	T	−	Fi/T
Prominent interphalangeal joints	+	28/35	−		−	−	−	−	−	+
Prominent distal phalanges	+	21/35	−		−	+	+	+	−	+
Scoliosis/spinal abnormalities	+	10/34		+		−	+	−	−	+
Joint laxity	−			+	+	−	+	+	−	+
Others										
Hirsutism	+		+	+	+	+	+	+	+	+
Congenital heart defects	−	6/34	TR,MR,AS	CoA, AtSD, VSD	CoA, AS, VSD	AtSD	−	−	−	+
Genitourinary defects	Cr, HS	13/20Cr,2/32VUR	−		HS, Cr	−	−	−	−	Cr
Gastrointestinal abnormalities	−				AA, RUF	IO, GER	−	−	−	−
Inguinal (I)/umbilical (U) hernia	I/U	14/35	−	−	−	I	−	−	−	−
Sucking difficulty	+		+	+	+	+	+	+	+	+
Feeding difficulty	+		+	+	+	+	+	+	+	+
Frequent vomiting	+									
Hearing impairment	+			+	−	+	−	+	−	−
Visual impairment	+			−			+	−	+	−
Recurrent infections	−	+	+	+	+	+	+	+	+	+

+, present; −, absent; blank, data not available; §, Tsurusaki et al. [2013]; #, SD score;†, SD acore; ‡, at latest assessment; AA, anal atresia; ACC, agenesis of corpus callosum; AS, aortic stenosis; ASD, autism spectrum disorder; AtSD, atrial septal defect; C, cleft palate; CH, cerebellar hypoplasia; CoA, coarctation of aorta; Colp, colpocephaly; Cr, cryptorchidism; DW, Dandy-Walker malformation; F, female; Fi, finger; GER, gastroesophageal reflux; H, high palate; HA, hyperactivity; HCC, hypoplastic corpus callosum; HS, hypospadias; Im, impulsiveness; IO, intestinal obstruction; M, male; MR, mitral regurgitation; NBS, Nicolaides-Baraitser syndrome; NW, no words; O, obsession; RUF, retrourethral fistula; T, toe; TR, tricuspid regurgitation; VSD, ventricular septal defect; VUR, vesicoureteral reflux; fractions in the previous publications show patient numbers "feature-positive/data available"

TABLE IC. Clinical Features of Patients With Mutations in the Components of SWI/SNF Complex

Gene	*ARID1B*					
Patient (subject no. in the previous report§)	5 (12)	n = 4	n = 8	n = 9	n = 6	n = 1
Age at publication (years of age)	19	11/12–4	3–46	3 3/12–20	2–40	2
Sex	M	2M,2F	2M,6F	4M,5F	1M,5F	M
Mutation	Del (9.2Mb)	Del (3.77–13.81Mb) [Nagamani et al., 2009]	7Del (0.2–14.5Mb),1Tra [Halgren et al., 2012]	1Del(2.5Mb),1Dup(exon 5/6),3Ns,4Fs [Hoyer et al., 2012]	3Del(0.73–2.72),2Ns,1Fs [Santen et al., 2012]	Del(1.19Mb) [Michelson et al., 2012]
Growth						
Prenatal growth (birth weight/length)#	−2.3/−3.7	3/4		0/9	0/6	−
Postnatal growth (weight/height)†	−2.3/−6.1	1/3	5/7	3/9	3/6	−
Psychomotor						
Developmental delay/mental retardation‡	Severe	4/4(2Moderate, 2Severe)	8/8	5Moderate,4Severe	2Moderate, 4Severe	Moderate
Speech delay	NW	4/4(3NW, 1SW)	8/8(3NW,5SW)	9/9(2NW, 2SW, 3Se)	6/6(2NW, 3Severe, 1Moderate)	NW
Seizures	+	1FC	3/6	3/9		
Hypotonia	−	2	7/8	7/9		+
Autistic features/behavioral abnormalities	HA		5/7	1	1	
Microcephaly (≤2 SD) (SD score)	+	4/4	1/6	2/9	0/6	−
Brain anomaly	−?	2/3(ACC + Colp)	4/5(1ACC, 3HCC, 1HCV)	0/6	4/4(3ACC, 1HCC, 2Colp)	HCC
Craniofacial						
Sparse hair	+		1	1	1	
Thick eyebrows	+		1		6/6	
Thick/long/prominet eyelashes	−					
Ptosis	−	1				
Abnormal ears	+	2	1	7/9		
Nasal bridge	Narrow	3Broad	3Broad			
Thick, anteverted alae nasi						Broad
Wide mouth	−		2	1		+
Philtrum	Long	2Long	2Long	1Long		
Upper lip vermilion feature		2Thin	3Thin,1Thick	6/9(6Thin)		Thin
Thick lower lip vermilion	−	2Thick	3			
Palatal abnormality	H	2H		2/9(2H)		
Skeletal-limb						
Hypoplastic/absent fifth finger/toe	Fi/T				2/6(2Fi)	
Hypoplastic/absent nail (fifth finger/toe)	+		1T	1T	2/6(2Fi)	
Hypoplastic/absent nail (other fingers/toes)				1?	1/6	
Prominent interphalangeal joints	+					
Prominent distal phalanges	−	1				
Scoliosis/spinal abnormalities	+		1	1		
Joint laxity	−		3/4		3/5	
Others						
Hirsutism	+		3/4	2		3/6
Congenital heart defects	MR	1AtSD	1AtSD	2/9(1AtSD)	1AtSD	
Genitourinary defects	−	1PSW	1Cr, 1DoUr, 2RL	2Cr, 1MU	1RL, 1DoUr	
Gastrointestinal abnormalities	GU, GER		1Co, 1AA	1AA		
Inguinal (I)/umbilical (U) hernia	−					
Sucking difficulty	−	3	4			+
Feeding difficulty	−		5	+		
Frequent vomiting						
Hearing impairment	−	4	1/2	1/9	+	
Visual impairment	−	1St, 1Am	2Hy, 2My, 2St,1 Cat, 1Ny		3St/9,4My	2St
Recurrent infections	+	1	1			

+, present; −, absent; blank, data not available; §, Tsurusaki et al. [2013]; #, SD score; †, SD acore; ‡, at latest assessment; AA, anal atresia; ACC, agenesis of corpus callosum; Am, amblyopia; AtSD, atrial septal defect; Cat, cataract; Co, constipation; Colp, colpocephaly; Cr, cryptorchidism; Del, deletion; Dup, duplication; DoUr, double ureter; F, female; Fi, finger; Fs, frameshift mutation; GER, gastrointestinal reflux; GU, gastric ulcer; H, high palate; HA, hyperactivity; HCC, hypoplastic corpus callosum; HCV, hypoplastic cerebellar vermis; Hy, hypermetropia; M, male; MR, mitral regurgitation; MU, megaureter; My, myopia; Ns, nonsense mutation; NW, no words; Ny, nystagmus; PSW, penoscrotal webbing; RL, renal lithiasis; Se, sentences; St, strabismus; SW, several words; T, toe; Tra, translocation; fractions in the previous publications show patient numbers "feature-positive/data available"

FIG. 1. Clinical photographs of patients with an *SMARCB1* mutation. SMARCB1-1: Craniofacial features at age 2 months (a), 1 year (b), 6 years (c), and 18 years (d). Note a round face with thick and arched eyebrows, a short nose with a bulbous tip and anteverted nostrils, a long philtrum, a small mouth, and micro-retrognathia in the early childhood. Later, note a broad nasal bridge without anteverted nostrils, a broad philtrum, a large tongue, and a protruding jaw. Poor posture due to severe scoliosis (e) as well as hypoplastic fingers (f, g) and toes (h, i) with nail hypoplasia, prominent interphalangeal joints, and prominent distal phalanges are noted at age 21 years. SMARCB1-3: Craniofacial features in the neonatal period (j, k), at age 2 years (l, m), and 7 years (n). Note a round face with thick and arched eyebrows, a short nose with anteverted nostrils, a long philtrum, a small mouth, and micro-retrognathia in early childhood. Later, note a broad nasal bridge and a protruding jaw. Feet at age 5 years (o, p). Note hypoplasia of the bilateral fifth toes and hypoplasia of all toenails. (Figure I originally published in Tsurusaki et al. [2012], in *Nature Genetics*.)

156 cm (−2.6 SD), and an OFC of 51.2 cm (−3.8 SD). He suffers from constipation, nocturnal enuresis, and unstable body temperature. He understands simple commands and speaks several words. He is friendly but also hyperactive and impulsive.

SMARCA4-3 (Subject 5 [Tsurusaki et al., 2012]; Fig. 2h–o): Increased nuchal translucency thickness was shown by fetal ultrasonography. He was born at 41 weeks of gestation. His birth weight was 2,756 g (−1.2 SD), length was 48 cm (−0.9 SD), and OFC was 32.0 cm (−0.9 SD). He was gavage-fed due to sucking/feeding difficulties until 7 months of age. He had right cryptorchidism which was corrected surgically at age 1 year. He showed hypotonia and motor development was delayed: he raised his head at age

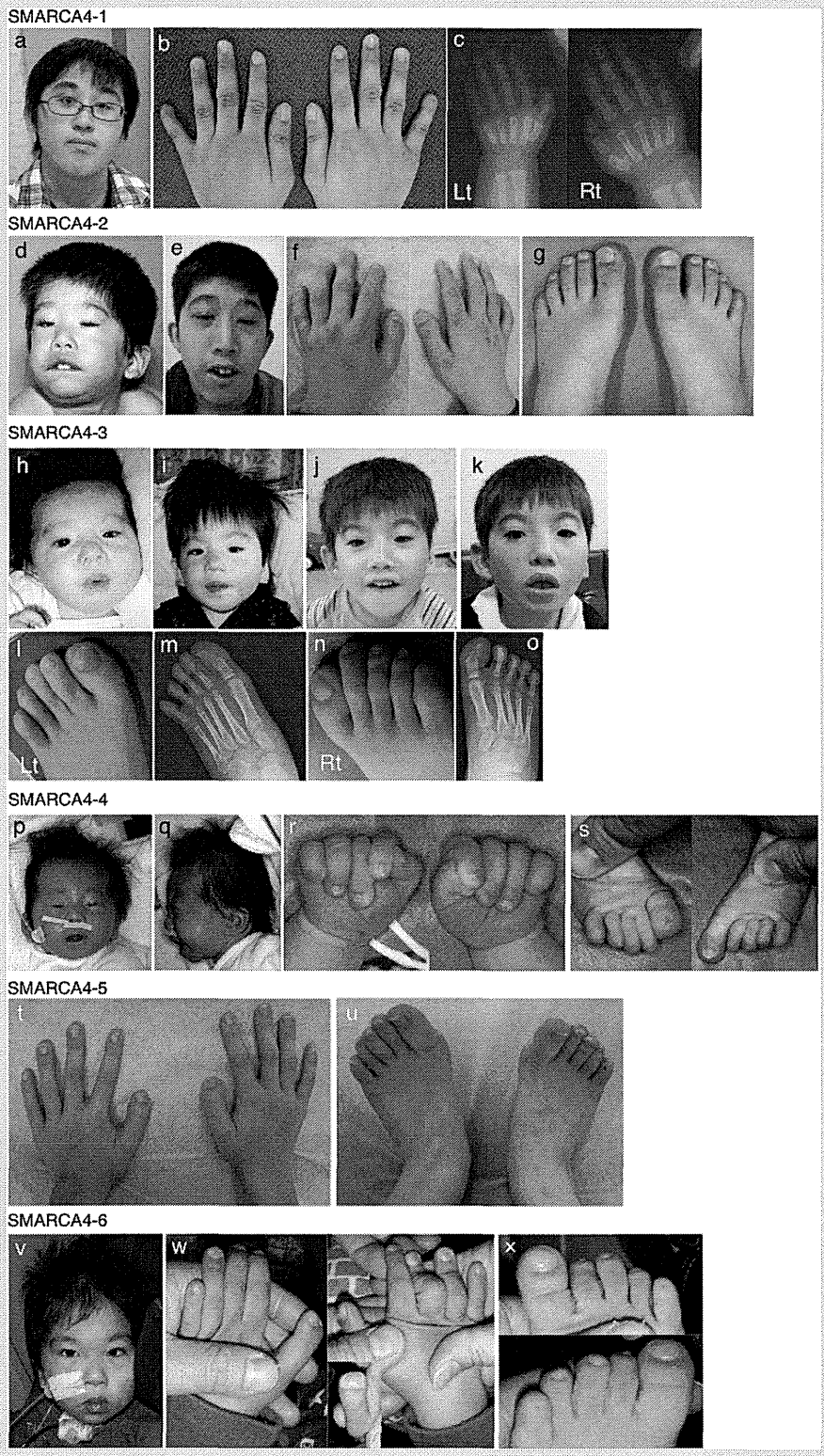
SMARCA4-1
a
b
c
Lt
Rt
SMARCA4-2
d
e
f
g
SMARCA4-3
h
i
j
k
l
Lt
m
n
Rt
o
SMARCA4-4
p
q
r
s
SMARCA4-5
t
u
SMARCA4-6
v
w
x

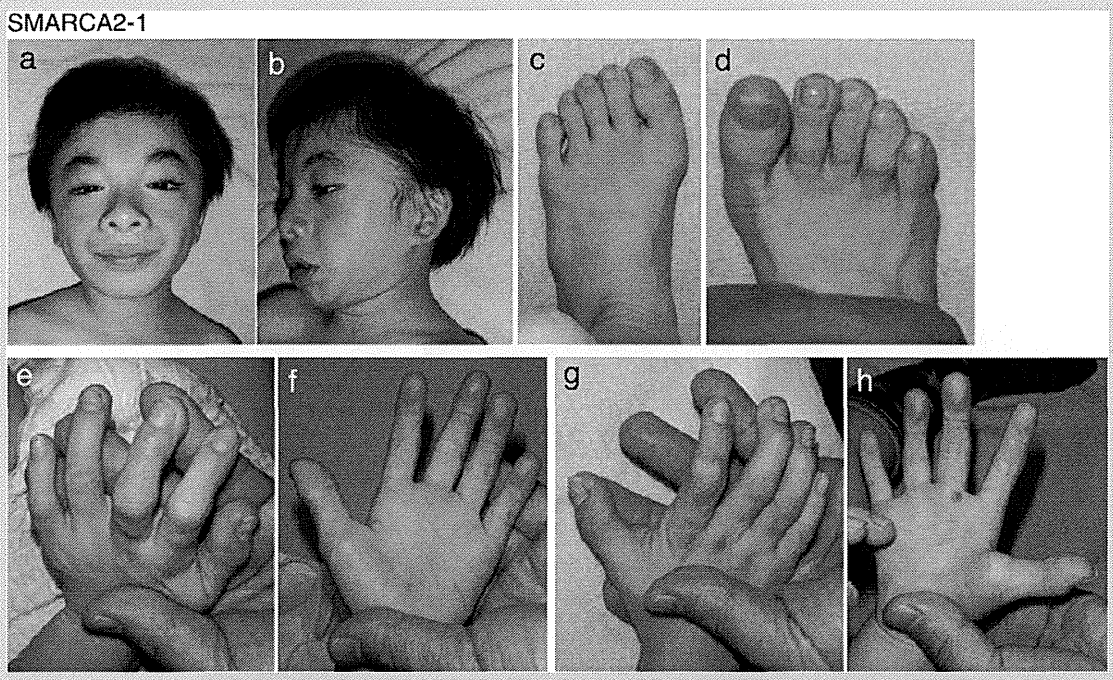

FIG. 3. Clinical photographs of a patient (SMARCA2-1) with an *SMARCA2* mutation. Craniofacial features (a, b), feet (c, d), and hands (e–h) at age 6 6/12 years. Note sparse hair, thick, and arched eyebrows, a broad nasal bridge with anteverted nostrils, a broad philtrum, a wide mouth, and thick upper and lower lip vermilions; and prominent interphalangeal joints and prominent distal phalanges of all fingers and toes without nail hypoplasia. (Figure a, d originally published in Tsurusaki et al. [2012], in *Nature Genetics*.)

7 months, sat alone at 1 3/12 years, and walked independently at 6 years. His developmental quotient (DQ) was 17 at age 5 9/12 years. MRI of the brain at age 6 11/12 years showed hypoplasia of the upper cerebellar vermis and mild hypoplasia of the corpus callosum. At age 9 10/12 years, he weighs 22.1 kg (−1.5 SD), has a height of 114 cm (−3.2 SD), and an OFC of 48 cm (−3.6 SD). He suffers from unstable body temperature, facial flushing, aerophagia, and intractable constipation. His skeletal problems have included bilateral genu recurvatum with an episode of patella dislocation, bilateral pes valgus, subluxation in the left hip, and Perthes disease-like changes in the right hip. He has autism spectrum disorder with hypersensitivity, hyperactivity, self-injurious behaviors, obsession,

FIG. 2. Clinical photographs of patients with *SMARCA4* mutations. SMARCA4-1: Craniofacial features (a) and hands (b) at age 18 years and hand radiographs (c) at age 5 months. Note a slender face with thick eyebrows, an everted upper lip vermilion, a protruding jaw; hypoplasia of bilateral distal phalanges of the first and fifth fingers, and bilateral hypoplastic fifth fingernails. SMARCA4-2: Craniofacial features at age 2 years (d) and 20 years (e). Note hypertrichosis, a narrow forehead, blephalophimosis that was corrected surgically, thick and slightly arched eyebrows, long eyelashes, a short and low nose with anteverted nostrils, a short philtrum, an everted upper lip vermilion, and low-set ears in the early childhood; and later a slender face with a long nose and a thick lower lip vermilion. Hands at age 20 years (f). Note hypoplasia of the distal phalanges and nails of bilateral fingers and prominent interphalangeal joints. Feet at age 20 years (g). Note prominent distal phalanges of bilateral first toes and hypoplasia of bilateral fifth toes as well as aplasia of bilateral fifth toenails. SMARCA4-3: Craniofacial features at age 4 months (h), 2 2/12 years (i), 5 1/12 months (j), and 9 10/12 years (k). Note arched eyebrows growing thicker, left ptosis, prominent ears, an everted upper lip vermilion, and a thick lower lip vermilion. Feet at age 9 10/12 years (l–o). Note prominent distal phalanges of bilateral first toes, hypoplasia of bilateral second-to-fifth toes, hypoplasia of bilateral fourth toenails, and aplasia of bilateral fifth toenails. SMARCA4-4: Craniofacial features (p, q), hands (r), and feet (s) in the neonatal period. Note a round face with thin and arched eyebrows, blephalophimosis, low-set ears, a thin upper lip vermilion, and micro-retrognathia; hypoplasia of bilateral fifth fingers and toes, aplasia of bilateral fifth fingernails and toenails, and hypoplasia of bilateral second-to-fifth fingernails and toenails. SMARCA4-5: Hands (t) and feet (u) at age 8 years. Note hypoplasia of bilateral fifth fingers and toes, hypoplasia of bilateral first and fifth fingernails and second-to-fifth toenails, prominent distal phalanges of bilateral first toes, and prominent interphalangeal joints. SMARCA4-6: Craniofacial features (v), hands (w), and feet (x) at age 3 7/12 years. Note thick and arched eyebrows and small mouths, hypoplasia of bilateral fifth fingers and toes, bilateral all fingernails and bilateral first-to-fourth toenails, aplasia of bilateral fifth toenails, and prominent distal phalanges of bilateral first toes. (Figure k, n, p, r originally published in Tsurusaki et al. [2012], in *Nature Genetics*.)